Title

A luciferase fragment complementation assay to detect focal adhesion kinase (FAK) signaling events

Journal

Heliyon, 9(4)

ISSN

1879-4378

Authors

Estep, Jason A

Sun, Lu O

Riccomagno, Martin M

Publication Date

2023-04-01

DOI

10.1016/j.heliyon.2023.e15282

Peer reviewed

Heliyon 9 (2023) e15282

Contents lists available at ScienceDirect

Heliyon

journal homepage: www.cell.com/heliyon

Research article

A luciferase fragment complementation assay to detect focal adhesion kinase (FAK) signaling events

Jason A. Estep [a], Lu O. Sun [c], Martin M. Riccomagno [a,b,*]

[a] Cell, Molecular and Developmental Biology Program, Department of Molecular, Cell and Systems Biology, University of California, Riverside, CA 92521, USA
[b] Neuroscience Program, Department of Molecular, Cell and Systems Biology, University of California, Riverside, CA 92521, USA
[c] Department of Molecular Biology, UT Southwestern Medical Center, Dallas, TX 75390, USA

ARTICLE INFO

Keywords:
Integrin adhesion complexes
Focal adhesions
Focal adhesion kinase
Integrin
Cell migration
Cell motility
Luciferase fragment complementation assay
Split luciferase

ABSTRACT

Integrin Adhesion Complexes (IACs) serve as links between the cytoskeleton and extracellular environment, acting as mechanosensing and signaling hubs. As such, IACs participate in many aspects of cellular motility, tissue morphogenesis, anchorage-dependent growth and cell survival. Focal Adhesion Kinase (FAK) has emerged as a critical organizer of IAC signaling events due to its early recruitment and diverse substrates, and thus has become a genetic and therapeutic target. Here we present the design and characterization of simple, reversible, and scalable Bimolecular Complementation sensors to monitor FAK phosphorylation in living cells. These probes provide novel means to quantify IAC signaling, expanding on the currently available toolkit for interrogating FAK phosphorylation during diverse cellular processes.

1. Introduction

Cell-Matrix adhesions are critical regulators of cellular motility and structure, tissue morphogenesis, anchorage-dependent growth, and cell survival [1–3]. Integrin Adhesion Complexes (IACs, or simply 'adhesion complexes') are the best studied examples of cellular-extracellular adhesions, serving to physically link the extracellular matrix (ECM) to the actin cytoskeletal system [2,4–7]. IACs are highly dynamic structures that encompass at least four types of adhesive complexes, each with distinct molecular compositions and signaling capacity. These include focal complexes (FXs, also referred to as nascent adhesions), focal adhesions (FAs), fibrillar adhesions (FBs), and cellular podosomes [8–10]. To date, proteomic approaches have identified over 200 IAC components, termed the 'integrin adhesome' [7,11–13], although a consensus set of 60 proteins organized into four signaling modules has been recently proposed [14, 15]. Additionally, adhesive complexes continually exchange components with the cytosol, allowing them to rapidly remodel in response to internal or external stimuli [16–18]. Given this molecular diversity and dynamism, IACs are able to act as signaling hubs, permitting mechanosensation of traction forces [19–21] and relaying anchorage-dependent growth and survival signals to the cell [22–25]. In addition, their regulated establishment and turnover are essential for processive cell migration, cellular podosome formation, and epithelial-to-mesenchymal transitions [26–28].

Due to their functions linking the extracellular environment to the cytoskeleton, IACs and the proteins that form them have been

Abbreviations: ECM, extracellular matrix; FA, focal adhesion; FAK, Focal Adhesion Kinase; FB, fibrillar adhesion; FX, focal complex; IAC, Integrin Adhesion Complexes; LFCA, Luciferase Fragment Complementation Assay.

* Corresponding author. Department of Molecular, Cell and Systems Biology, University of California, Riverside, CA 92521, USA.
E-mail address: martinmr@ucr.edu (M.M. Riccomagno).

https://doi.org/10.1016/j.heliyon.2023.e15282
Received 13 July 2022; Received in revised form 29 March 2023; Accepted 31 March 2023
Available online 5 April 2023

shown to be involved in many aspects of development and disease [7,29–39]. Many of these structural and signaling functions of IACs are mediated through Focal Adhesion Kinase (FAK), a nonreceptor tyrosine kinase that is recruited to the inner plasma membrane upon integrin receptor clustering and ECM engagement [40–46]. Increased FAK expression and kinase activity have been associated with cancer cell survival, the formation of invadopodia, and tumor progression [47–56]. Conversely, FAK deficiency in mice results in embryonic lethality [34], with cellular defects in IAC turnover, cell migration, and growth factor response [57–60]. Phospho-regulation of FAK has emerged as a central theme in coordinating FAK activity, and extensive studies have elucidated the biochemical regulation of FAK during IAC assembly and turnover. A key phosphorylated FAK residue is Tyr-397, which is trans-autophosphorylated upon integrin receptor stimulation and FAK oligimerization [41–43,61–65], allowing subsequent associations with Src-Homology 2 (SH2) domain containing partners [61,66–69]. FAK recruitment and autophosphorylation of Tyr-397 are some of the earliest observable steps in IAC assembly [4,41,70,71] and overexpression of mutant Y397F-FAK results in longer IAC occupancy times and inhibited IAC turnover in migrating cells [60,72]. Following Tyr-397 phosphorylation, full activation of FAK is achieved by Src-mediated phosphorylation of Tyr-576 and Tyr-577 residues within the kinase domain activation loop [66,73,74]. These modifications destabilize inhibitory interactions between the *N*-terminal FERM domain and the *C*-terminal catalytic domain, resulting in a more open conformation and full FAK kinase activity [75–78]. Previous studies have demonstrated that mutating these three tyrosine residues to phenylalanine (Y397-576-577F) reduces FAK *in vitro* kinase activity to 20% of wildtype levels [79]. Collectively, these studies demonstrate that phospho-regulation of these tyrosine residues is essential in regulating FAK kinase activity, making these post-translational modifications attractive targets for monitoring IAC signaling events.

While several methodologies have been developed to monitor FAK conformational changes and activity using florescent imaging probes [72,76,80–89], we sought to develop simple and reliable sensors that would detect FAK tyrosine phosphorylation without the need for advanced microscopy. Bi-molecular Complementation Assays (also called Split-Reporter Assays) have emerged as powerfully adaptable genetically-encodable tools that allow for live-cell monitoring of diverse molecular, cellular, and physiological processes

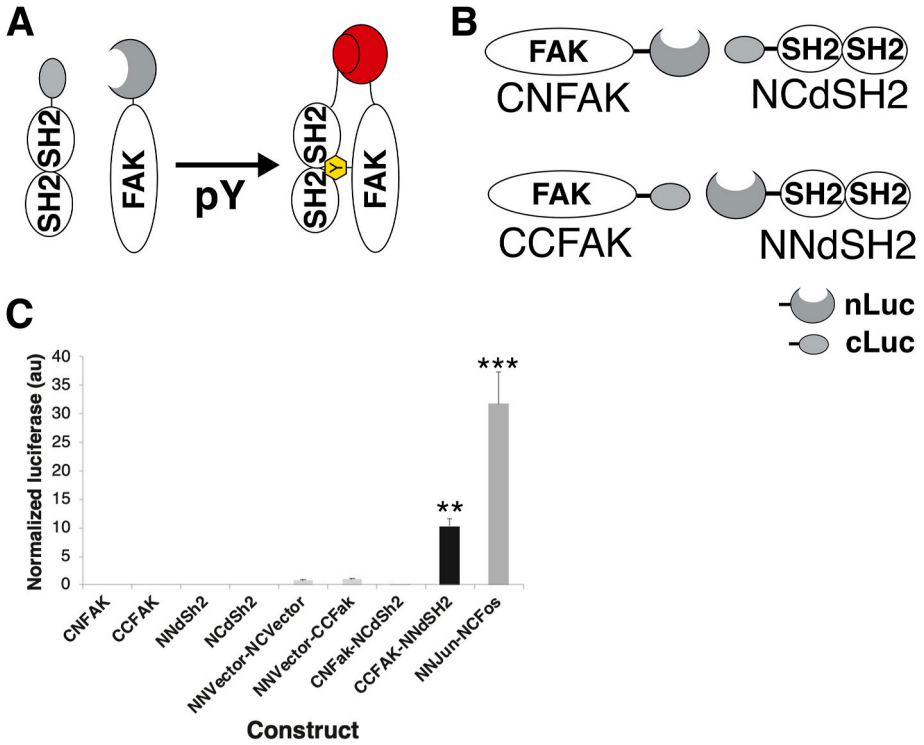

Fig. 1. Design of pYFAK BiLuc constructs. (**A**) Schematic representation of pYFAK BiLuc general approach. Intramolecular interactions between phosphotyrosine-FAK (pYFAK) and a phosphotyrosine sensor (double SH2, dSH2) permit reconstitution of enzymatically active firefly luciferase. (**B**) Design of pYFAK split luciferase construct pairs. The first letter of the construct name describes the attachment point of split luciferase fragments on FAK and dSH2 interaction targets (*N*-terminal vs *C*-terminal), while the second letter indicates which fragment of split luciferase was attached at this position. nLuc: *N*-terminal Luciferase (aa1-416) depicted as a grey crescent; cLuc: *C*-terminal Luciferase (aa401-550) depicted as a grey oval. (**C**) Tests of different pyFAK split luciferase construct pairs in HEK293 cells identify an effective pyFAK probe pair (CCFAK + NNdSH2; pYFAK BiLuc) which displays high specificity and low background activity. Individual constructs (CNFAK, CCFAK, NNdSH2, NCdSH2) do not produce detectable luciferase activity, nor do untethered luciferase constructs when co-transfected (NNVector + NCVector). Similarly, luciferase activity is dependent on the presence of both FAK and dSH2 interaction partners (NNVector + CCFAK). The activity of a previously described split-luciferase reporter system (NNJun + NCFos) is shown for comparison. Renilla luciferase was co-transfected as a control in all cases. Luciferase activity is normalized to baseline firefly/renilla luciferase ratio of the NNVector + CCFAK pair (ANOVA $p < 0.01$, followed by Tukey Post-hoc **$p < 0.01$; ***$p < 0.001$ compared to baseline; $N = 4$).

[90–92]. Conceptually, these systems comprise of a reporter that is rendered undetectable by genetic dissection into complementary fragments, which are separately tethered to putative interacting proteins. These split reporters are often a fluorescent molecule [93], or a luminescent [94] or colorimetric enzyme [90]. Associations between interaction targets results in spontaneous reassembly of the reporter molecule and generation of a detectable signal. Split luciferase systems, also termed Luciferase Fragment Complementation Assays (LFCAs), enjoy widespread use in both basic and preclinical settings due to their unrivaled sensitivity, rapid assembly and disassembly kinetics, amenability to *in vivo* and *in vitro* systems, and low costs of implementation [95,96]. Here, we present the design and characterization of novel luciferase-based Bi-molecular Complementation probes to quantify FAK tyrosine phosphorylation during IAC signaling events in living cells. We find these tools faithfully report IAC signaling in a manner that is sensitive and dynamic along physiologically relevant timescales. These tools have the potential to be scalable for screening purposes, and as such will be a valuable addition to the expanding toolkit to monitor FAK activity and IAC dynamics.

2. Results

To monitor FAK tyrosine phosphorylation (pYFAK) events, we designed a bimolecular luciferase (BiLuc) system that pairs a

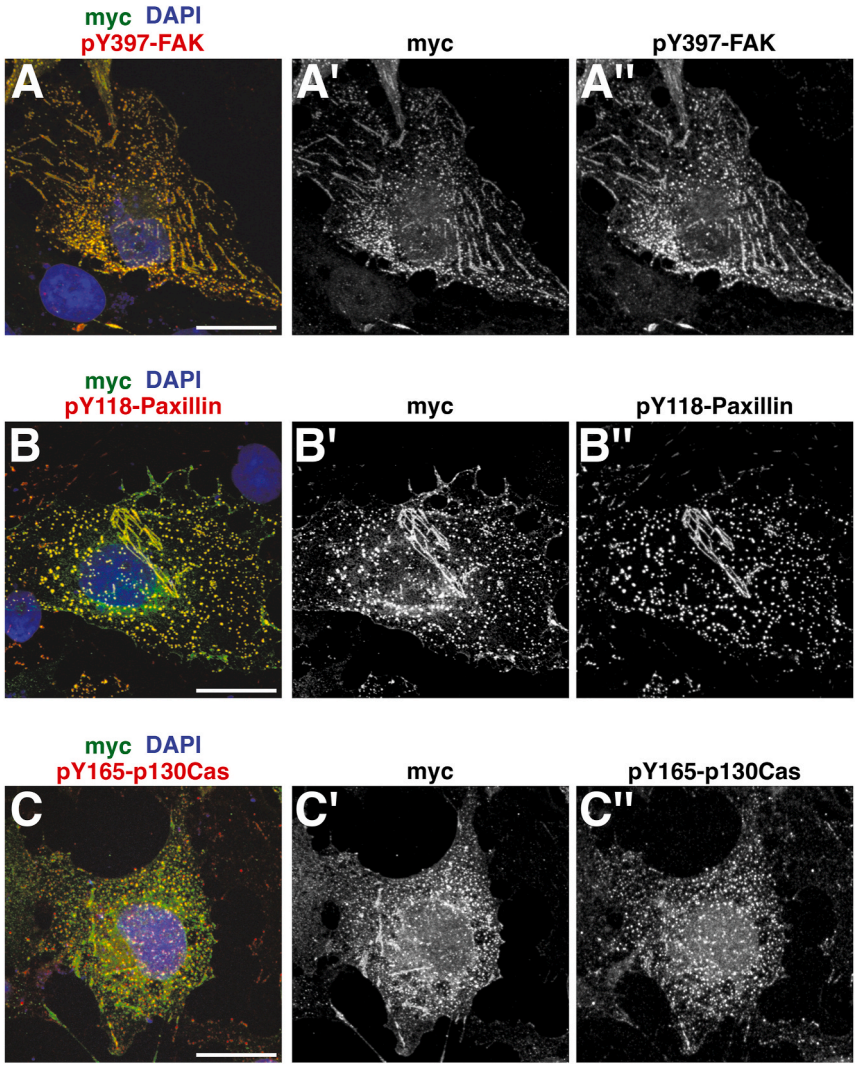

Fig. 2. pYFAK BiLuc constructs are recruited to actively signaling FAs. (**A-C″**) Immunofluorescence for myc (green) and IAC phosphoproteins (green) in COS-7 cells transfected with pYFAK BiLuc constructs. Colocalization analysis confirms myc-tagged FAK constructs (green) incorporate into actively signaling IAC. Strong correlation is observed between myc **(A,A′)** and pY397-FAK **(A,A″)** (Pearson's R = 0.77 ± 0.02 and Spearman's rank correlation ρ = 0.83 ± 0.01) indicating the CCFAK construct is incorporating into adhesion complexes. Similar correlation is observed between myc **(B,B′)** and pY118-Paxillin **(B,B″)** (R = 0.73 ± 0.10 and Spearman's rank correlation ρ = 0.77 ± 0.09), another early marker of active FAs. Correlation is weaker between myc (**C,C′**) and pY165-P130Cas (**C,C″**) (Pearson's R = 0.40 ± 0.02 and Spearman's rank correlation ρ = 0.57 ± 0.02). Scale bar = 20 μm for all. See also Figure S1.

Table 1
Colocalization analysis between myc-tagged CCFAK probe and IAC phosphomarkers.

	Pearson's R								
	myc/Y397-FAK			myc/Y165-p130Cas			myc/Y118-Paxillin		
	Average	Standard Dev	SEM	Average	Standard Dev	SEM	Average	Standard Dev	SEM
CCFAK + NNdSH2									
BR#1	0.754375	0.114190994974793		0.42	0.129083306434256		0.735833333333333	0.117817912925246	
BR#2	0.797857142857143	0.039453686856787		0.383333333333333	0.145418935034839		0.828	0.0654871852240683	
BR#3	0.766666666666667	0.0470055721114403		0.394666666666667	0.138866156869878		0.628461538461538	0.0883030910978544	
Total	0.77296626984127	0.0224151274138771	0.0129413798463217	0.399333333333333	0.0187735037871049	0.0108388874651175	0.628461538461538	0.0998657385456197	0.0576575110321343
CCFAK-3YF + NNdSH2									
BR#1	0.808666666666667	0.0425720677484774		0.380588235294118	0.163808831670742		0.690769230769231	0.0810824208713511	
BR#2	0.806428571428571	0.0640441125447792		0.51	0.0935414346693484		0.79625	0.0750888362763289	
BR#3	0.752142857142857	0.0946392804632076		0.408	0.13586758259423		0.455	0.113257550420591	
Total	0.789079365079365	0.0320075222640161	0.0184795515952226	0.432862745098039	0.0681943420045254	0.0393720217135221	0.647339743589744	0.174721151817703	0.100875304035072
	Spearmann's Rank								
	myc/Y397-FAK			myc/Y165-p130Cas			myc/Y118-Paxillin		
	Average	Standard Dev	SEM	Average	Standard Dev	SEM	Average	Standard Dev	SEM
CCFAK + NNdSH2									
BR#1	0.817487811875	0.0970103252849545		0.54448519117647	0.115875056614123		0.741131895833333	0.0691774011646073	
BR#2	0.841215224285714	0.0350919815474262		0.588627456666667	0.0929136175992199		0.866142279333333	0.0613853660428348	
BR#3	0.819023437333333	0.0645591525434268		0.572157997333333	0.0949164848264663		0.701001373076923	0.0754250562261802	
Total	0.825908824498016	0.0132779494739478	0.00766602770307001	0.568423548392157	0.0223068259132139	0.0128788519457602	0.769425182747863	0.0861293346840556	0.0497267945649629
CCFAK-3YF + NNdSH2									
BR#1	0.860349940666667	0.0325834120945256		0.524344712352941	0.0953094184692931		0.728821200769231	0.0593671301524598	
BR#2	0.864741255714286	0.0377422363681278		0.634866276	0.0487705550051456		0.84355305875	0.0452193349024428	
BR#3	0.811851324285714	0.0773052673713638		0.562197952666667	0.0901231111383378		0.600183786666667	0.106035503975448	
Total	0.845647506888889	0.0293505942166799	0.0169455734718756	0.573802980339869	0.0561672636703941	0.0324281847997467	0.724186015395299	0.121750828975334	0.0702928738829693

phospho-tyrosine sensor with rapid luciferase assembly and disassembly kinetics to produce a sensitive, reversible reporter of FAK activation (Fig. 1A). In this system, complementary *C*-terminal (cLuc, aa401-550) and *N*-terminal (nLuc, aa1-415) fragments of firefly luciferase enzyme [94] are tethered by flexible RSIAT (Arg-Ser-Ala-Ile-Thr) linker sequences to *c*-myc tagged FAK and to a phospho-tyrosine sensor, respectively. This phospho-tyrosine sensor consists of a double repeat of Src Homology 2 motifs (double SH2, or dSH2) derived from pp60 (*c*-Src), which has been previously shown to display high affinity for tyrosine-phosphorylated targets in IACs, including FAK, Paxillin, and p130Cas [82,97,98]. Tyrosine phosphorylation of FAK is detected by direct binding of the dSH2 sensor, thereby allowing the *N*- and *C*-terminal fragments of luciferase to reassemble into a catalytically active enzyme (Fig. 1A).

To explore different configurations for the split-luciferase constructs, we designed two alternate pYFAK split-luciferase pairs by tethering either *N*- or *C*-terminal fragments of firefly luciferase enzyme to the *C*-terminal of a myc-taged FAK coding sequence (CNFAK and CCFAK, respectively) and complementary luciferase fragments to the *N*-terminal of the dSH2 phospho-tyrosine sensor (NCdSH2 and NNdSH2, respectively) (Fig. 1B). We determined only one pair of constructs (CCFAK + NNdSH2) was able to reconstitute firefly luciferase enzymatic activity (Fig. 1C), and subsequent experiments were carried out using this set. This pair is hereafter referred to as pYFAK BiLuc. Importantly, the split luciferase fragments alone display no detectable enzymatic activity without the interaction of the FAK-dSH2 fusion products, as neither individually transfected constructs (CNFAK, CCFAK, NNdSH2, NCdSH2) nor co-transfected but untethered luciferase fragments (NNVector-NCVector) were able to produce notable luminescent activity in transfected HEK293 cells (Fig. 1C).

To determine if the CCFAK construct was incorporated into IACs in the context of the pYFAK BiLuc sytem *in vivo*, we transfected these constructs into COS-7 cells grown on laminin-coated coverslips. We then performed immunocytochemistry to detect the *N*-terminal myc tag in the CCFAK probe (Fig. 2; Figure S1). In all cases, we observe the myc tag robustly labels small, peripheral Focal Contacts (FXs), Focal Adhesions (FAs) and larger, elongated fibrillar bodies (FBs) (Fig. 2A′,B′,C′) [8,10]. The identity of these structures is confirmed by co-labeling with pY397-FAK (Fig. 2A-A″) and pY118-Paxillin (Fig. 2B–B″). Interestingly, pY165-p130Cas co-labeled some FXs and FAs, but not all, and is absent from larger FBs (Fig. 2C–C″), consistent with previous descriptions of this scaffolding protein being present in nascent FXs and FAs, but not more mature FBs [9]. To quantify the degree of pYFAK BiLuc incorporation into IACs, we performed whole-cell colocalization analysis between the myc-tagged CCFAK probe and the forementioned phosphoproteins. Colocalization analysis revealed strong correlation between myc and pY397-FAK (Fig. 2A-A″, Table 1) (Pearson's $R = 0.77 \pm 0.02$ and Spearman's rank correlation $\rho = 0.83 \pm 0.01$). Similarly, strong correlation is observed between myc and pY118-Paxillin (Fig. 2B–B″, Table 1) (Pearson's $R = 0.73 \pm 0.10$ and Spearman's rank correlation $\rho = 0.77 \pm 0.09$). A weaker correlation was observed between myc and pY165-P130Cas (Fig. 2C–C″, Table 1) (Pearson's $R = 0.40 \pm 0.02$ and Spearman's rank correlation $\rho = 0.57 \pm 0.02$), possibly reflecting the more restricted localization of this phosphoprotein. Collectively, these results confirm efficient recruitment of pYFAK BiLuc probes to various actively signaling IAC structures.

Next, we sought to evaluate if the pYFAK BiLuc system was functionally responsive to endogenous integrin signaling events. Extensive studies have established the Src family of kinases as the primary kinases responsible for phosphorylating FAK Y576-577 residues during IAC signaling events *in vivo*, leading to full activation of FAK kinase activity [42,66,74]. Pharmacological treatment of cell lines with the Src-family kinase inhibitors PP2 or SU6665 results in a notable reduction of FAK phosphorylation [99–101]. Therefore, it was expected that luciferase activity from the pYFAK BiLuc system would be proportionally responsive to the degree of Src kinase activity in the cell. Indeed, we found that treatment with the Src-family kinase inhibitor PP2 resulted in progressively

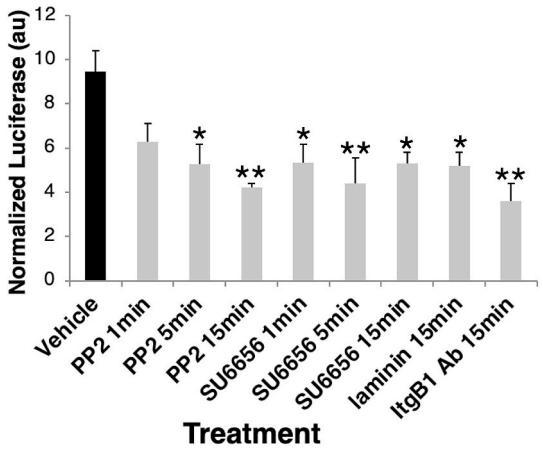

Fig. 3. pYFAK BiLuc constructs respond to pharmacological blocking of adhesion signaling. Quantification of pYFAK BiLuc (CCFAK + NNdSH2) enzyme activity following treatments with adhesion signaling blocking agents. Signal was normalized to baseline firefly/renilla luciferase ratio of untreated NNVector + CCFAK pair. Application of 10 μM PP2 results in a progressive reduction in luciferase activity following application, with a 33% reduction after 1 min (NS), 43% reduction after 5 min, and maximal repression of 55% after 15 min. Application of SU6656 results in a significant 43% drop in luciferase activity after 1 min, 54% after 5 min, and return to 43% reduction after 15 min. A 15 min incubation with Ha2/5 integrin-β1 function blocking antibody (ItgB1 Ab) results in a 61% decrease in luciferase activity compared to vehicle treatment ($N = 4$; ANOVA $p < 0.01$, followed by Tukey Post-hoc *$p < 0.05$; **$p < 0.01$). Error bars = SEM.

diminished luciferase reporter activity in transfected HEK293 cells, with a maximal decrease of 55.6% observed after 15 min incubation (Fig. 3; ANOVA $p < 0.01$; Tukey Post-hoc test $p < 0.05$ 5 min vs control; $p < 0.01$ 15 min vs control; $n = 4$). Similar levels of inhibition were observed after only 1 min incubation with the Src-family inhibitor SU6656 (Fig. 3; $p < 0.05$ 1 min vs control; $p < 0.01$ 5 min vs control; $p < 0.05$ 15 min vs control). Importantly, Src family kinases may be activated by several endogenous pathways and therefore result in FAK phosphorylation independent of integrin receptor activity. Integrin-β1 is one of only 3 Integrin-β subunits expressed in this cell line (Human Protein Atlas, proteinatlas.org [102]). Therefore, to address if the pYFAK BiFC system was also responsive to integrin receptor activity, cells were treated with an integrin-β1 function blocking antibody (Ha2/5) [103] and luciferase signal was measured. Treated cells displayed a robust 61.8% reduction in normalized luciferase signal 15 min following Ha2/5 addition to the culture medium (Fig. 3; $p < 0.01$ vs control), confirming that the pYFAK BiLuc system is sensitive to both Src family

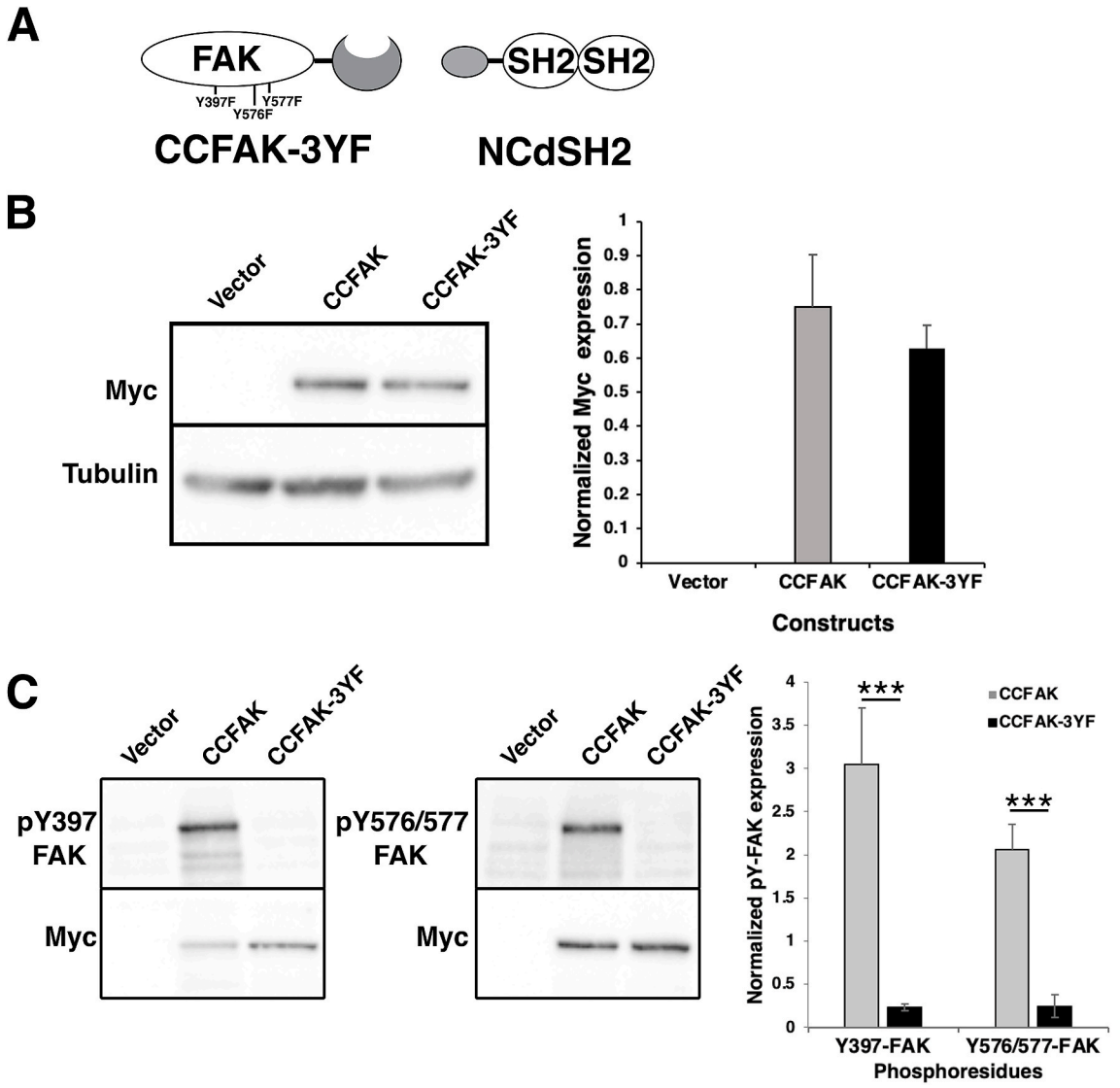

Fig. 4. Design and expression of the phospho-mutant CCFAK-Y3F. (**A**) Schematic representation of the three-point mutations introduced to produce the CCFAK-YF construct. Tyrosine to phenylalanine missense mutations were introduced to tyrosine residues Y397, Y576, and Y577. (**B**) Western Blot of transfected HEK293 cells showing robust myc signal from both CCFAK and CCFAK-3YF transfected cells. 20 ng of total protein was ran for each lane. Right panel, quantification of myc expression normalized to tubulin levels ($N = 3$ biological replicates; Mann-Whitney *U* test: $p = 1$; $U = 5$). **(C)** Western Blot and quantification from HEK293 cells transfected with pCDNA3.1-myc/his (Vector), CCFAK, or CCFAK-3YF constructs. Separate membranes were blotted for either pY397-FAK or pY576/577-FAK, stripped and reblotted for myc and tubulin. Quantification of pY397-FAK and pY576/577-FAK intensity normalized to myc levels are presented; we observe a 13-fold reduction in pY397-FAK intensity and 8-fold reduction in pY576/577-FAK intensity in the CCFAK-3YF transfected cells (*t*-test *$p < 0.0001$ for all; $N = 4$ biological replicates). 5 μg of total protein loaded per lane, error bars represent standard error of the mean (SEM). For uncropped versions of the Western blots see Figures S2 (related to **4B**) and **S3** (related to **4C**).

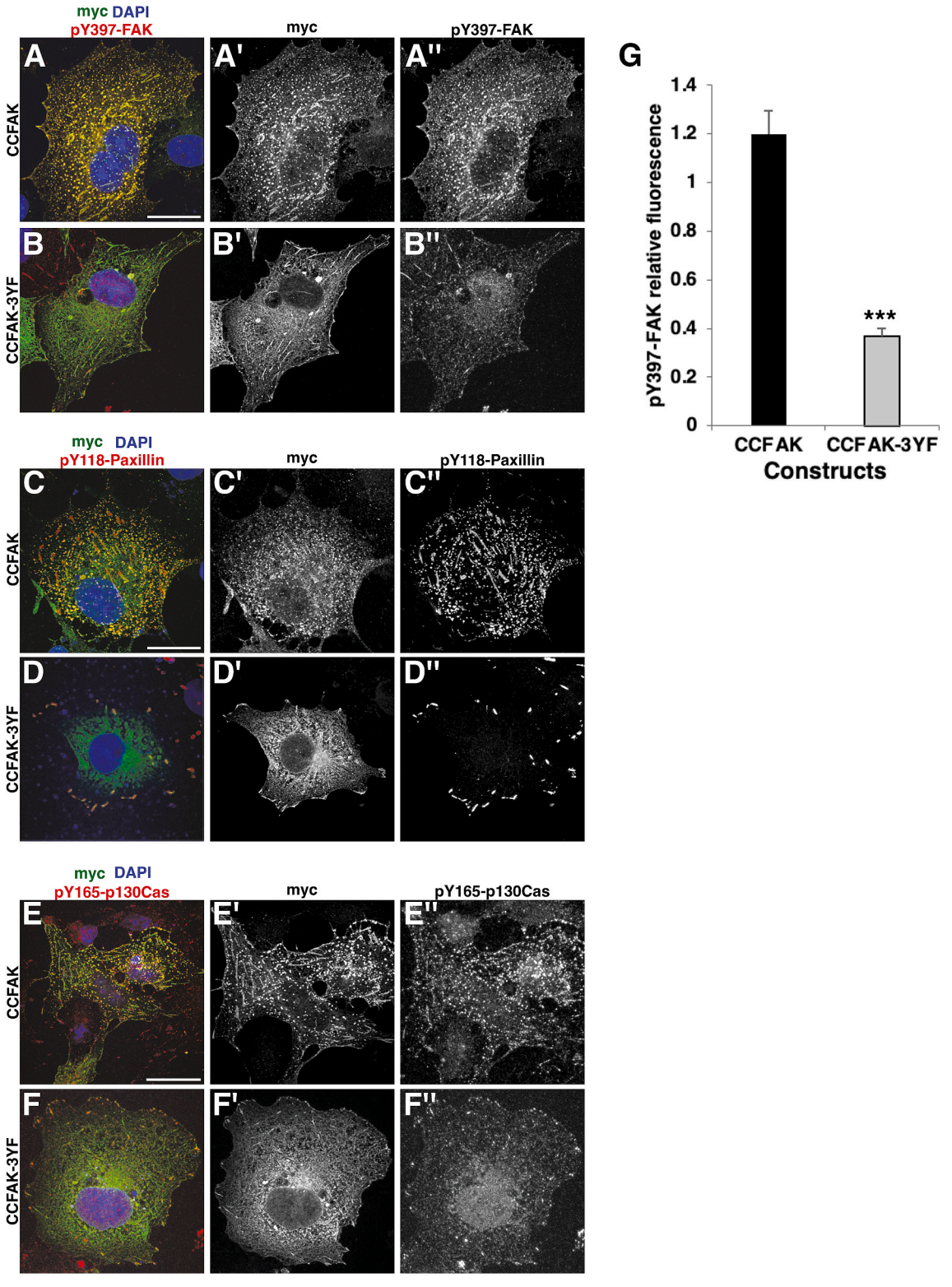

(caption on next page)

Fig. 5. pYFAK BiLuc recruitment to IAC **is not dependent on tyrosine phosphorylation**. (**A-F″**) Immunofluorescence for myc-tagged FAK constructs (green) and IAC phosphoproteins (green) in transfected COS-7 cells. Colocalization analysis confirms myc-tagged CCFAK-3YF construct incorporates into actively signaling IAC in transfected COS-7 cells, as revealed by phospho-specific antibodies (red). Moderate correlation is observed between myc **(A,A′, B, B′)** and pY397-FAK **(A″,B″)** (Mander's M1 = 0.62 ± 0.12 and Spearman's rank correlation ρ = 0.46 ± 0.07) indicating the CCFAK-3YF construct half is incorporating into IAC. Similar correlation is observed between myc **(C,C′, D, D′)** and pY118-Paxillin **(C″,D″)** (M1 = 0.41 ± 0.1 and Spearman's rank correlation ρ = 0.31 ± 0.06), another early marker of active FAs. Correlation is also somewhat weak between myc and pY165-P130Cas (***E*-F″**) (M1 = 0.52 ± 0.07 and Spearman's rank correlation ρ = 0.38 ± 0.06). Scale bar = 20 μm for all. **(G)** Quantification of relative pY397-FAK fluorescence normalized to myc levels for cells transfected with CCFAK and CCFAK-3YF (N = 11 and 14 cells, two-tailed *t*-test ***p < 0.001). Grey bars CCFAK; Black bars CCFAK-3YF. Error bars represent standard error of the mean (SEM).

activity and endogenous integrin receptor activation. These results also demonstrate the reversibility of the luciferase signal, along the order of minutes, in response to pharmacological treatment, which mirrors IAC assembly and turnover rates observed in live imaging studies [70,82,104]. These data suggest the pYFAK BiLuc system could indeed be applicable for quantifying changes in steady-state levels of adhesion signaling in response to other pharmacological perturbations, or in the design of genetic screens.

The dSH2 phospho-tyrosine sensor used in this design has previously been shown to also display affinity for other IAC phospho-tyrosine species, including the core scaffolding proteins Paxillin and p130Cas [70,82,97,98]. To directly test the specificity of the pYFAK BiLuc system towards FAK tyrosine phosphorylation events, we designed an alternate CCFAK construct that contains tyrosine-to-phenylalanine point mutations at the three key tyrosine residues regulating FAK kinase activity: Y397, Y576 and Y577 (CCFAK-3YF) [73,79] (Fig. 4A). We thoroughly characterized the expression CCFAK-3YF before carrying out the reconstitution experiment. We started by confirming robust expression of the CCFAK-3YF probe by Western blot using antibodies to detect the myc tag (Fig. 4B, uncropped image of blots in Fig. S2). This expression is comparable to that of WT CCFAK (N = 3 biological replicates; Mann-Whitney *U* test: p = 1; U = 5) (Fig. 4B). We then tested whether the 3 tyrosine-to-phenylalanine point mutations introduced to create the CCFAK-3YF construct abolished phosphorylation of these residues. HEK293T cells were transfected with WT CCFAK or CCFAK-3YF, and Western blot analysis was then carried out to detect pY397-FAK and pY576/Y577-FAK. As expected, the mutations in CCFAK-3YF notably and significantly reduced phosphorylation in those residues compared to WT CCFAK (Fig. 4C, uncropped image of blots in Fig. S3): a 13-fold reduction in normalized pY397-FAK intensity and 8-fold reduction in pY576/577-FAK intensity were observed in the CCFAK-3YF transfected cells as compared to CCFAK-transfected cells (two-tailed unpaired *t*-test p < 0.0001 for both comparisons; N = 4 biological replicates).

To confirm this reduction in phosphorylation and determine whether CCFAK-3YF was recruited to IACs, we performed immunocytochemistry for myc and the core IAC phosphoproteins pY397-FAK, pY118-Paxillin, and pY165-p130Cas (Fig. 5). Similarly to the unmodified CCFAK probe (Fig. 2; Fig. 5A-A″,C–C″,*E*-E″), we observe the myc tag of the CCFAK-3YF probe labels FXs, FAs, and larger, elongated FBs (Fig. 5B–B″,D-D″,F–F″). Whole cell colocalization analysis showed a moderate correlation between myc and pY397-FAK (Fig. 5B–B″, Table 2) (Mander's M1 = 0.62 ± 0.12 and Spearman's rank correlation ρ = 0.46 ± 0.07). This is consistent with the inability of CCFAK-3YF of being phosphorylated in that residue, that results in an overall reduction of pY397-FAK in cells transfected with CCFAK-3YF vs. CCFAK (70% decrease N = 11–14 cells; two-tailed *t*-test p < 0.001**; Fig. 5**G). The correlation between myc and pY118-Paxillin is even lower **(Fig. 5**D-D″, **Table 2)** (M1 = 0.41 ± 0.1 and Spearman's rank correlation ρ = 0.31 ± 0.06). Again, a moderate correlation was observed between myc and pY165-P130Cas (Fig. 5F–F″, Table 2) (M1 = 0.52 ± 0.07 and Spearman's rank correlation ρ = 0.38 ± 0.06). These correlations were found to be significantly different from those measured for the CCFAK construct (Fig. 2, Tables 1 and 2) (N = 3 biological replicates; Mann-Whitney *U* test; $p = 3.99 \times 10^{-11}$ for myc/pY397-FAK; $p = 3.44 \times 10^{-9}$ for myc/pY118-Paxillin; $p = 5.26 \times 10^{-8}$ for myc/pY165-p130Cas). Overall, these data indicate that although the CCFAK-3YF can be recruited to actively signaling IACs, it does so less efficiently, likely as a result of this construct not being properly phosphorylated and therefore unable to phosphorylate downstream players.

Finally, to test whether FAK phosphorylation on residues Y397, Y576 and Y577 is required for the interaction between the FAK and dSH2 probes, we co-transfected WT CCFAK or CCFAK-3YF with NNdSH2 and measured luciferase activity as above (Fig. 6). Notably, we observed an almost complete attenuation of luciferase activity in CCFAK-3YF + NNdSH2 transfected HEK293 cells (90.36% reduction; N = 4 biological replicates; Mann-Whitney *U* test: p = 0.0285) (Fig. 6). Since this marked reduction in luciferase signal cannot be ascribed to a decrease in overall CCFAK-3YF expression (Fig. 4), it can thus be concluded that this diminishment is the result of abolishing pYFAK-dSH2 interactions. Collectively, these data confirm that the pYFAK BiLuc system is specific and sensitive to the relative levels of FAK tyrosine phosphorylation.

3. Discussion

In this study we made use of the bimolecular complementation approach to design a sensitive, specific reporter of FAK tyrosine phosphorylation, a posttranslational modification that has emerged as a critical regulator of IAC signaling [41,69,105,106]. Based on the system's reliance on bimolecular complementation of firefly luciferase (BiLuc) and demonstrated specificity toward tyrosine phosphorylated FAK (pYFAK) (Figs. 4 and 6), we term this tool the pYFAK BiLuc system. To our knowledge, this is the first luciferase-based reporter system developed to monitor FAK activation during IAC signaling events.

3.1. pYFAK BiLuc design, specificity, and sensitivity

In approaching the design of a sensor that specifically recognizes FAK tyrosine phosphorylation, we chose to take advantage of the

Table 2
Colocalization analysis between myc-tagged CCFAK or CCFAK-3YF and IAC phosphomarkers.

	Spearman's Correlation		Mander's M1		Mander's M2	
	myc/Y397-FAK		myc/Y397-FAK		myc/Y397-FAK	
	CCFAK + NNdSH2	CCFAK-3YF + NNdSH2	CCFAK + NNdSH2	CCFAK-3YF + NNdSH2	CCFAK + NNdSH2	CCFAK-3YF + NNdSH2
Sample average	0.825382	0.458032	0.958733	0.622344	0.967444	0.622
Sample size	45	32	45	32	45	32
Sample SD	0.0708131	0.0667912	0.0490224	0.128818	0.0619144	0.198604
Median	0.8353114	0.4600813	0.968	0.5965	0.98	0.617
Skewdness	−2.155618	−0.12791	−4.666881	0.240178	−5.720134	0.0452621
Normality	0.000005998	0.441	2.34E-10	0.1089	3.35E-12	0.4011
Outliers	0.52894466, 0.63860952		0.674, 0.897, 0.904		0.582, 0.922	
Outlier count	2	0	3	0	2	0
Rank	2471	532	2466	537	2423.5	579.5
U	4	1436	9	1431	51.5	1388.5
P-value	1.41E-13		2.06E-13		4.93E-12	
Z	7.3956		7.3446		6.9077	
Standard Effect Size	0.84		0.84		0.79	
Common Language Effect Size	1		0.99		0.96	

	Spearman's Correlation myc/Y118-Paxillin		Mander's M1 myc/Y118-Paxillin		Mander's M2 myc/Y118-Paxillin	
	CCFAK + NNdSH2	CCFAK-3YF + NNdSH2	CCFAK + NNdSH2	CCFAK-3YF + NNdSH2	CCFAK + NNdSH2	CCFAK-3YF + NNdSH2
Sample average	0.774968	0.309043	0.925256	0.410324	0.938231	0.382216
Sample size	40	37	39	37	39	37
Sample SD	0.0991264	0.0542955	0.113973	0.103998	0.0667578	0.0979589
Median	0.773633529999999	0.29736128	0.966	0.391	0.956	0.365
Skewdness	−0.275383	0.898396	−2.538997	−0.195274	−1.507802	0.560994
Normality	0.0172	0.03199	1.38E-08	0.06294	0.00002932	0.00002932
Outliers		0.46484483	0.533, 0.539, 0.67, 0.741		0.731, 0.743	
Outlier count	0	1	4	0	2	0
Rank	2300	703	2214	712	2223	703
U	0	1480	9	1434	0	1443
P-value	4.75E-14		1.33E-13		6.57E-14	
Z	7.5396		4.4037		7.4964	
Standard Effect Size	0.86		0.85		0.86	
Common Language Effect Size	1		0.99		1	

	Spearman's Correlation myc/Y165-p130Cas		Mander's M1 myc/Y165-p130Cas		Mander's M2 myc/Y165-p130Cas	
	CCFAK + NNdSH2	CCFAK-3YF + NNdSH2	CCFAK + NNdSH2	CCFAK-3YF + NNdSH2	CCFAK + NNdSH2	CCFAK-3YF + NNdSH2
Sample average	0.562378	0.380564	0.727581	0.523176	0.725	0.498059
Sample size	38	34	43	34	43	34
Sample SD	0.103341	0.0674917	0.135241	0.0699799	0.147963	0.144218
Median	0.57599749	0.407437579999999	0.743	0.522	0.741	0.5165
Skewdness	0.104829	−0.941922	−0.235448	0.87346	−0.472569	0.657026
Normality	0.2458	0.00197	0.01918	0.1678	0.08722	0.01101
Outliers				0.759		0.218, 0.989
Outlier count	0	0	0	1	0	2
Rank	1973	655	2253.5	749.5	2208	795
U	60	1232	154.5	1307.5	200	1262
P-value	3.99E-11		3.44E-09		5.26E-08	
Z	6.6045		5.9089		5.4422	
Standard Effect Size	0.78		0.67		0.62	
Common Language Effect Size	0.95		0.89		0.86	

Src Homology 2 (SH2) domain of pp60 (c-Src), as this domain mediates the interaction between FAK and Src during adhesion signaling events [61,67]. Indeed, other groups have used probes derived from the Src SH2 domain to investigate IAC dynamics and monitor phosphotyrosine accumulation in a variety of contexts [18,80,82,97,107–115]. Many of these probes, including the pYFAK BiLuc system presented here, make use of a double tandem repeat of the Src SH2 domain (dSH2), an approach originally developed in Dr. Benny Geiger's laboratory at the Weitzmann Institute [82,97]. Importantly, in the initial report this dSH2 sensor was shown to have

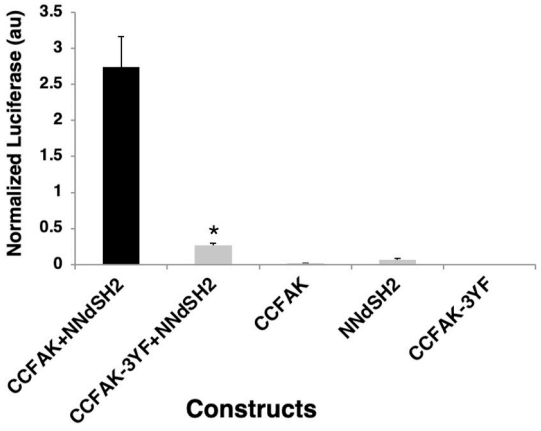

Fig. 6. pYFAK BiLuc signal is dependent on specific FAK tyrosine residues. Quantification of pyFAK BiLuc enzyme activity for tested constructs. Luciferase activity is normalized to baseline firefly/renilla luciferase ratio of the NNdSH2 (Mann-Whitney *U* test *p = 0.02857 compared to CCFAK + NNdSH2, N = 4). Error bars represent standard error of the mean (SEM).

broad binding ability to pY residues in adhesion complexes, displaying a linear correlation with an *anti*-pY antibody and demonstrating the capability of co-precipitating both p130Cas and paxillin [82]. This observation of broad affinity of the dSH2 sensor to several phosphotyrosine species in adhesion complexes has been reproduced by subsequent users, and exploited by some in the design of FRET-based assays to examine interactions between multiple adhesion complex components or monitor phosphotyrosine content during adhesion signaling events [76,97]. However, this broad affinity for phosphotyrosine species presents a challenge in designing a tool that is specific to FAK tyrosine phosphorylation, but insensitive to the phosphorylation status of other adhesion components. Therefore, we chose to incorporate the dSH2 sensor into a bi-molecular complementation design.

Bi-molecular complementation systems (also called split reporter systems) are powerful programmable tools due to their modular nature and ability to be genetically encoded. These systems often display high specificity, as the split reporter approach requires the stoichiometric balance, proximity, and proper orientation of both putative interaction targets to reconstitute reporter signal [91,92,116]. As applied to the detection of tyrosine phosphorylated FAK, we reasoned that tethering the two halves of a reporter molecule to the dSH2 sensor and to FAK itself would permit reporter reconstitution only in adhesive complexes where FAK and Src interact [42,67,68,117], in a phosphorylation-dependent manner [61,63,69], generating the specificity we desired. Indeed, we show that only one pair of split-luciferase constructs designed and tested was able to reconstitute luciferase activity (Fig. 1C), suggesting that the luciferase fragments cannot drive self-reassembly and that proper relative positioning mediated by pYFAK-dSH2 interactions is essential for reporter activity. Reconstitution of luciferase activity is dependent on the presence of both the dSH2 and FAK products, as untethered luciferase fragments are unable to spontaneously reassemble into functional enzyme when co-transfected (NNVector-NCVector, Fig. 1C); nor can a soluble nLuc fragment spontaneously associate with the FAK-cLuc fusion product when co-expressed (NNVector-CCFAK, Fig. 1C). We go on to demonstrate the specificity of the pYFAK BiLuc system to FAK tyrosine phosphorylation, as mutation of three key regulatory tyrosine residues to phenylalanine (Y397-576-577 F) [79] nearly completely abolishes luciferase activity (Fig. 6). This strong attenuation of luciferase signal is unlikely to be explained by loss of recruitment to IACs alone. While statistical analysis revealed significant differences in the colocalization of each of the pYFAK BiLuc construct (CCFAK vs CCFAK-3YF) with the three IAC components pY397-FAK, pY118-Paxillin, and pY165-p130Cas, a moderate correlation between these IAC markers and CCFAK-3YF is still observed (Fig. 5, Table 2). These results are in partial accordance with previous studies that have shown that mutating tyrosine residues on FAK, or pharmacological blocking of the FAK-Src complex, does not alter IAC composition, but does affect signaling properties and cellular phenotypes [72,87,118,119]. Collectively, these results indicate that the pyFAK BiLuc system presented is highly specific to FAK phosphorylation, and not responsive to other resident IAC phosphoproteins.

When designing a bi-molecular complementation system, the investigator must carefully consider the benefits and limitations of the reporter molecule chosen. Here, we chose to make use of a split-luciferase reporter because of the high sensitivity, signal-to-noise ratio, and rapid assembly and disassembly kinetics these split-reporter enzymes provide [95,96,120]. In contrast to split-fluorescent systems, where reassembly of the reporter is irreversible due to the high intrinsic stability of the reconstituted fluorophore [92,116], split-luciferase systems demonstrate ready reversibility [94,121–123]. Importantly, this ensures that the observable signal reflects steady-state associations between interaction targets and avoids potential experimental artifacts stemming from the production of interaction target aggregates, which may result in the cellular accumulation signaling complexes, resulting in above physiological-levels of activity. We find that pYFAK BiLuc signal is rapidly attenuated, in the order of minutes, by pharmacological block of Src-family kinases or with incubation of an integrin-β1 function blocking antibody (Fig. 3). These results demonstrate that the pYFAK BiLuc system is responsive along IAC disassembly and turnover timescales [70,82,104], while confirming that these tools are responsive to the endogenous integrin receptor signaling axis. Additionally, we note that the degree of luciferase attenuation by pharmacological block of Src family kinases (maximal 55.6% reduction after 15 min of PP2 treatment, Fig. 3) or antibody-mediated block of integrin receptor (61.8% reduction with 15 min Ha2/5 treatment, Fig. 3) is not as dramatic as the near complete abolishment

of luciferase activity observed by mutating the three regulatory tyrosine residues to phenylalanine (Y397-576-577 F) (CCFAK + NNdSH2 vs. CCFAK-3YF + NNdSH2, Figs. 4 and 6). During IAC assembly, engagement of ECM ligands induces integrin receptor clustering and recruitment of FAK, which in turn transautophosphorylates residue Y397, providing a docking site for Src kinase [41,45,46,61,67]. Therefore, it is possible that the residual luciferase activity observed after pharmacological treatment reflects dSH2 sensor binding to pY397-FAK, as this tyrosine phosphorylation event would still be expected to occur in the presence of PP2 or SU6665. Similarly, FAK may still be recruited to adhesive complexes in a cell that expresses a heterogenous population of integrin receptors, as the Ha2/5 antibody only targets one class (integrin-β1 subunit) of receptor complexes [103]. Notably, expression data accessed from the Human Protein Atlas (proteinatlas.org) indicates expression of 11 integrin receptor subunits by HEK293 cells: integrin-α2 (*ITGA2*), integrin-α3 (*ITGA3*), integrin-α4 (*ITGA4*), integrin-α5 (*ITGA5*), integrin-α6 (*ITGA6*), integrin-α7 (*ITGA7*), integrin-α8 (*ITGA8*), integrin-αV (*ITGAV*), integrin-β1 (*ITGB1*), integrin-β3 (*ITGB3*), and integrin-β5 (*ITGB5*) [102]. As such, 10 known heterodimer receptor combinations may potentially be formed in HEK293 cells, 8 of which include the integrin-β1 receptor subunit (αVβ3 and αVβ5 being the two exceptions). We speculate that the residual luciferase signal observed following Ha2/5 treatment may represent the fraction of integrin receptor complexes unaffected by this function-blocking monoclonal antibody, or simply an inability of the antibody to target all available integrin-β1 receptor complexes available. Collectively, we propose these observations demonstrate the sensitivity of the pYFAK BiLuc system to detect varying degrees of FAK tyrosine phosphorylation *in vivo*, and suggest it may therefore be applied to quantitatively measure, by proxy, the strength of IAC signaling [42,79].

3.2. Comparison to benchmark and potential applications

Traditional methodologies for monitoring phosphorylation in IACs include western blotting, co-immunoprecipitation experiments, and immunofluorescence using antibodies to detect particular phosphotyrosine residues [74,98]. For live-cell analysis, dSH2-YFP and dSH2-CFP constructs were developed by Dr. Benny Geiger's laboratory [82], and have since been employed for standard fluorescence imaging, as well as FRET-based and FRAP-based assays to monitor phosphotyrosine accumulation during IAC assembly and component exchange with the cytosol [76,87,97]. As technology advanced, several approaches designed to specifically target FAK functions or interactions were developed. The first were fluorescent-fusion proteins that allowed live-cell monitoring of FAK recruitment to IACs, and have been used to investigate the role of tyrosine phosphorylation in adhesion turnover [60,72,81]. A bimolecular fluorescence complementation (BiFC) approach was later developed to monitor interactions between FAK and Src-family kinases Src and Syk during IAC assembly [83]. Led by several lines of research indicating an important regulatory interaction between the *N*-terminal FERM domain and *C*-terminal catalytic domain [77,124,125], several groups developed FRET-based probes to investigate FAK intramolecular rearrangements and partner coupling during adhesion assembly [76,84,86]. More recently, fluorescent-based biosensors were developed to monitor FAK kinase activity *in vivo*, again using FRET-based biosensors that would change conformation in response to FAK-mediated phosphorylation [85,88], or by monitoring the differential fluorescence decay rates of a FAK phosphorylation-dependent biosensor [89]. These various approaches have contributed greatly to our understanding of FAK regulation and function during IAC assembly and signaling, yet none have permitted a simple, quantitative, scalable approach to monitor FAK phosphorylation and IAC signaling.

For these reasons, we aimed to fill an apparent gap in the literature by designing a Luciferase Fragment Complementation Assay (LFCA) to detect FAK phosphorylation. Whereas the above approaches have relied on genetically encoded fluorescent reporters, we felt that the inherit limitations of these systems prevent their widespread adoption in basic research and translational/preclinical settings. While these systems bring many benefits for multiplexing with other cellular markers and visualizing sub-cellular interactions, split-fluorescent and FRET-based systems are relatively insensitive to discrete signaling events, often requiring overexpression of interaction targets to detect appreciable signal [116]. Similarly, FRET-based and split-fluorescent reporters display large background signal, resulting in a comparatively poor signal-to-noise ratio [96]. Further, FRET and split-fluorescent systems are poorly translated to *in vivo* models, and require expensive, specialized microscopy equipment and computational analysis to process. In contrast, luciferase reporters display outstanding signal-to-noise ratio, as neither luciferase fragment produce bioluminescence, and the reconstituted enzyme requires investigator-supplied substrate for signal development [96,126]. Split-luciferase reporters display high dynamic range, over several orders of magnitude, and permit repeat measurements from a biological sample without worry of signal degradation, lending themselves to quantitative applications where both sensitivity and scale are desired [96]. Finally, split-luciferase reporters are relatively easy to measure, requiring a more accessible luminometer or plate reader, and have been successfully translated into *in vivo* models [96,127].

The before mentioned advantages of the pYFAK BiLuc system will likely make it useful for basic research and pre-clinical settings where the monitoring of FAK activation is desirable. In recent years, FAK has gained considerable attention for its potential roles in tumorigenesis or metastasis [51,52,128–131], given its established roles in mediating adhesion signaling and its integration with growth factor response pathways [22–24,118]. FAK has been found to be overexpressed in numerous human cancers [54,55,132–135] and its activity has been correlated with the development of the formation of invasive podosomes and increased cellular motility and proliferation [48–53,56,136]. As such, methods to inhibit FAK recruitment and kinase activity have been suggested as a therapeutic approaches in treating cancer progression and metastasis [129,130,137–140]. While many of the associations between FAK and cancer progression have been established by comparing gene or protein expression from tumor biopsies, a robust method to monitor FAK activity *in vivo* remained lacking. We believe the pYFAK BiLuc system represents a first-in-its-class approach to monitoring FAK tyrosine phosphorylation and IAC signaling. A limitation of our study is that we have not established the kinetics of luciferase assembly for these probes. However, our data demonstrate that the pYFAK BiLuc system is responsive to IAC signaling inhibition along IAC disassembly and turnover timescales (Fig. 3) [70,82,104]. Collectively, our results indicate that the pyFAK BiLuc system is a dynamic,

specific, and sensitive reporter of FAK activation, with the potential to be expanded for high-throughput drug screens, genetic screens, or other *in vivo* or *in vitro* applications to monitor cellular behavior. Our hope is that these tools will add versatility to the existing toolkit to monitor IAC dynamics in both basic research and preclinical/translational settings.

4. Materials and methods

4.1. Plasmids

Generation of the split Luciferase backbones: The split Luciferase backbones were generated by cloning the nLuc and cLuc split fragments into pCDNA3.1+. NNVector (containing nLuc) was generated by amplifying the nLuc fragment from pGL2-Basic (Promega) using the following primers: F:CCCGGATCCACCATGGAAGACGCCAAAAACATAAAG; R:CCCCTCGAGTGAATTCGCGGCCGCCGTG GCGATGGAGCGTCCATCCTTGTCAATCAAGGCG. The amplified fragment was then cloned into pCDNA3.1+ using the *Bam*HI-*Xho*I sites. NCVector (containing cLuc) was generated by PCR amplifying cLuc using the following primers: F: CCCTCTA-GACCGGCCTGCAAGATCCCGAACGACCTGAAACAGAAGGTCATGAACCACTCCGGTTATGTAAACAATCCGGAAG; R: GAAGGGCCCC-TACACGGCGATCTTTCCGCCCTTC. The amplified fragment was then subcloned into pCDNA3.1+ using the *Xba*I-*Apa*I sites.

Generation of CCFAK: CCFAK was generated by subcloning *N*-terminal myc-tagged FAK into NCVector. We first amplified *N*-terminal Myc-tagged FAK from pRcCMV-FAK-ntMyc (kindly provided by S.K. Hanks) using the following oligos: F: CCCTAAGCGGCCGCGAATTCAATGGAGCAGAAGCTGATCTCCG; R:CGCTCTAGAGTGTGGCCGTGTCTGCCCTAG. The amplified fragment was then subcloned into NCVector using the *Not*I-*Xba*I sites. The CCFAK-3YF construct was generated by Vector builder using CCFAK as a template.

Generation of dSH2 phosphotyrosine sensor: The SH2 domain from pp60 (*c*-Src) was amplified by PCR from embryonic cDNA two independent times using the following primers: for SH2a F:CCCTAAGCGGCCGCGAATTCAACCATGGGGAGCAACTATGTGGCGC CCTCC; R:GCGGGATCCTACGGTAGTGAGGCGGTGACAC; for SH2b F:GCGGGATCCAGCAACTATGTGGCGCCCTCC; R:CGCTCTAGA-TACGGTAGTGAGGCGGTGACAC. The resulting amplicons were combined and cloned by 3-way ligation into a NdCGFP backbone construct using the EcorI and *Xba*I sites. The NdCGFP backbone was previously generated by PCR amplification *C*-terminal EGFP and PEST domain of pd2EGFP-Basic (Clontech) using the following primers: F:CCCGGATCCGCCATGGGGAAGAACGGCATCAAGGTGAAC; R:CCCCTCGAGTGAATTCGCGGCCGCCGTGGCGATGGAGCGCACATTGATCCTAGCAGAAGC and subcloning into pCDNA3.1+ using the *Bam*HI/*Xho*I sites.

Generation of NNdSH2: NNdSH2 was generated by amplifying the dSH2 sequence from NdCGFP using the following primers: F: CCCTAAGCGGCCGCGGGAGCAACTATGTGGCGCCCTCC; R:CGCGGGCCCTACGGTAGTGAGGCGGTGACAC, and subcloning into the *Not*I-*Apa*I sites of the NNVector. All pYFAK BiLuc constructs will be deposited at Addgene.

4.2. Luciferase assays

HEK293 cells were seeded at 9.6 × 10 [3] cells/ml in tissue culture treated 96-well flat-bottom plates and co-transfected with pYFAK BiLuc constructs and pRL-TK at 24 h s using Lipofectamine 2000 (ThermoFisher) following manufacturer's instructions. A total of 130 ng DNA was transfected per well (60 ng each split construct and 10 ng pRL-TK control). Cultures were allowed to express for a subsequent 36 h s before lysis and measurement. Luciferase was measured in a GloMax 20/20 Luminometer (Promega) using the Dual Luciferase Kit (Promega) following manufacturer's instructions. Pharmacological treatment was performed immediately before passive lysis with PLB buffer for luminescence detection. Drugs were diluted to 10 μM final concentration in prewarmed culture media prior to addition to the cells. Treatment with vehicle for 15 min was used as control. Firefly luciferase activity was normalized to Renilla Luciferase activity. Four independent experiments were quantified for all treatments.

4.3. Immunocytochemistry and colocalization analysis

COS-7 cells were seeded at 5.7e4 cells/well in a 24-well plate on glass coverslips that had been coated overnight with a solution of 10 μg/ml laminin. Each well was co-transfected with 1 μg DNA per well (500 ng of each half construct: 500 ng CCLucFAK + 500 ng NNLucdSH2 or 500 ng CCLucFAK-3YF + 500 ng NNLucdSH2) using Lipofectamine 2000 (ThermoFisher) reagent in a 1 μg DNA:2 μl Lipofectamine 2000 ratio. Cells were allowed to express for 24 h after transfection before fixation with 4% paraformaldehyde in 1xPBS for 5 min at room temperature (RT). Coverslips were then blocked/permeabilized for 20 min at RT in a solution of 10% goat serum in 1xPBST (1xPBS+0.1%TritonX-100). Following blocking, coverslips were incubated in primary antibody overnight at 4C with gentle agitation. Coverslips were then washed for 4 10 min washes in 1xPBS prior to secondary antibody incubation for 3 h at RT. Coverslips were washed again for 4 10 min washes in 1xPBS before mounting with Flourogel + DABCO mounting medium. All primary antibodies were diluted at 1:250 and all secondary antibodies were diluted at 1:1000 in 1xPBS+5% goat serum. Antibodies used: mouse *anti*-myc (9e10, Cell Signaling Technologies, cat # 2276 S), rabbit *anti*-p130CasY165 (Cell Signaling Technologies, cat # 4015 S), rabbit *anti*-PaxillinY118 (Cell Signaling Technologies, cat # 69363 S), rabbit *anti*-FAKY397 (ThermoFisher, cat # 44624G), alexafluor 488 goat anti-mouse (ThermoFisher, cat # A-11001), alexaflour 647 goat anti-rabbit (ThermoFisher, cat # A-21244). Three independent transfections were quantified for colocalization analysis, and 10–15 cells were analyzed per condition. Confocal scanning images were acquired on a Leica DMi8 using an oil-immersion 63× objective (NA = 1.3) with a 1.85× digital zoom and z-stack acquired with 40–50 steps of sizes of 0.15 μm. Correlations of individual cells were calculated from maximally projected images. Individual cells were selected by manually drawing a ROI around the cell perimeter in FIJI, and auto-thresholding. Mander's M1 and M2 and Spearman's

rank ρ correlations were calculated using the Coloc2 plugin.

4.4. Western blot

HEK293 Cells were grown to 80% confluency in 6-well format and transfected with 4 μg DNA per well using Lipofectamine 2000 (ThermoFisher) reagent in a 1 μg DNA:2 μl Lipofectamine 2000 ratio. Cells were allowed to express for 24 h after transfection before being washed once in RT 1xPBS and collected in an NP-40 Lysis buffer containing 1 μM sodium orthovanadate, 1 μM PMSF, 1 μM sodium fluoride, and protease inhibitor cocktail, diluted following manufacturer instructions (Millipore Sigma, cat #P2714). Lysates were cooked at 95C for 10 min in 1× Laemmli buffer and 10 ng total protein was loaded per lane. Membranes were blotted for myc (clone 9e10, Cell Signaling Technologies, cat # 2276 S), pY397-FAK (ThermoFisher, cat # 44624G), pY576/577-FAK (Cell Signaling, cat # 3281s), or tubulin (Cell Signaling, cat # 2146 S). Secondary antibodies were goat anti-rabbit IgG HRP-linked (Cell Signaling, cat # 7074 S) and goat anti-mouse IgG, HRP-linked (Cell Signaling, cat # 91196 S). All antibodies were diluted 1:1000 in 1xTBST+5%BSA and signal developed using Radiance Plus substrate (Azure Biosystems, cat # AC2103). pY397-FAK and pY576/577 signal was normalized to tubulin in all analyses.

4.5. Data analysis

Datasets were tested for normality using the Shapiro-Wilk test and QQ plot. This was followed by One-way ANOVA with Tukey's multiple comparisons test. For experiments that failed to meet normality, Mann-Whitney *U* test (with Bonferroni correction when appropriate) was performed.

Author contribution statement

Jason A. Estep: Conceived and designed the experiments; Performed the experiments; Analyzed and interpreted the data; Wrote the paper.

Lu O. Sun: Conceived and designed the experiments; Performed the experiments; Analyzed and interpreted the data; Contributed reagents, materials, analysis tools or data.

Martin Riccomagno: Conceived and designed the experiments; Performed the experiments; Analyzed and interpreted the data; Contributed reagents, materials, analysis tools or data; Wrote the paper.

Funding statement

Dr. Martin Riccomagno was supported by National Institute of Neurological Disorders and Stroke {R01NS104026}.

Lu O. Sun was supported by National Eye Institute {R00EY029330} and Southwestern Medical Foundation.

Dr. Martin Riccomagno was supported by Cancer Research Coordinating Committee {CRN19585662}.

Data availability statement

Data included in article/supp. Material/referenced in article.

Declaration of interest's statement

The authors declare that they have no known competing financial interests or personal relationships that could have appeared to influence the work reported in this paper.

Acknowledgements

We would like to acknowledge Dr. S.K. Hanks for the pRcCMV-FAK-ntMyc construct. We would also like to thank Alyssa Treptow for technical support. Finally, we would like to thank Dr. Patrick Kerstein for critically reading the manuscript, and Dr. Alex Kolodkin for his generosity.

Appendix A. Supplementary data

Supplementary data to this article can be found online at https://doi.org/10.1016/j.heliyon.2023.e15282.

References

[1] B. Wehrle-Haller, Assembly and disassembly of cell matrix adhesions, Curr. Opin. Cell Biol. 24 (5) (2012) 569–581, https://doi.org/10.1016/j.ceb.2012.06.010.

[2] B. Geiger, Cytoskeleton-associated cell contacts, Curr. Opin. Cell Biol. 1 (1) (1989) 103–109, https://doi.org/10.1016/S0955-0674(89)80045-6.
[3] D.R. Critchley, Focal adhesions - the cytoskeletal connection, Curr. Opin. Cell Biol. 12 (1) (2000) 133–139, https://doi.org/10.1016/S0955-0674(99)00067-8.
[4] S. Miyamoto, H. Teramoto, O.A. Coso, et al., Integrin function: molecular hierarchies of cytoskeletal and signaling molecules, J. Cell Biol. 131 (3) (1995) 791–805, https://doi.org/10.1083/jcb.131.3.791.
[5] B.M. Jockusch, P. Bubeck, K. Giehl, et al., The molecular architecture of focal adhesions, Annu. Rev. Cell Dev. Biol. 11 (1) (1995) 379–416, https://doi.org/10.1146/annurev.cb.11.110195.002115.
[6] K. Burridge, K. Fath, T. Kelly, G. Nuckolls, C. Turner, Focal adhesions: transmembrane junctions between the extracellular matrix and the cytoskeleton, Annu. Rev. Cell Biol. 4 (1988) 487–525, https://doi.org/10.1146/annurev.cb.04.110188.002415.
[7] S.E. Winograd-Katz, R. Fässler, B. Geiger, K.R. Legate, The integrin adhesome: from genes and proteins to human disease, Nat. Rev. Mol. Cell Biol. 15 (4) (2014) 273–288, https://doi.org/10.1038/nrm3769.
[8] B. Geiger, K.M. Yamada, Molecular architecture and function of matrix adhesions, Cold Spring Harbor Perspect. Biol. 3 (5) (2011) 1–21, https://doi.org/10.1101/cshperspect.a005033.
[9] M. Vicente-Manzanares, A.R. Horwitz, Adhesion dynamics at a glance, J. Cell Sci. 124 (23) (2011) 3923–3927, https://doi.org/10.1242/jcs.095653.
[10] C.D. Nobes, A. Hall, Rho, Rac, and Cdc42 GTPases regulate the assembly of multimolecular focal complexes associated with actin stress fibers, lamellipodia, and filopodia, Cell 81 (1) (1995) 53–62, https://doi.org/10.1016/0092-8674(95)90370-4.
[11] R. Zaidel-Bar, B. Geiger, The switchable integrin adhesome, J. Cell Sci. 123 (9) (2010) 1385–1388, https://doi.org/10.1242/jcs.066183.
[12] R. Zaidel-Bar, S. Itzkovitz, A. Ma'ayan, R. Iyengar, B. Geiger, Functional atlas of the integrin adhesome, Nat. Cell Biol. 9 (8) (2007) 858–867, https://doi.org/10.1038/ncb0807-858.
[13] A. Byron, J.D. Humphries, M.D. Bass, D. Knight, M.J. Humphries, Proteomic analysis of integrin adhesion complexes, Sci. Signal. 4 (167) (2011) 1–5, https://doi.org/10.1126/scisignal.2001827.
[14] E.R. Horton, P. Astudillo, M.J. Humphries, J.D. Humphries, Mechanosensitivity of integrin adhesion complexes: role of the consensus adhesome, Exp. Cell Res. 343 (1) (2016) 7–13, https://doi.org/10.1016/j.yexcr.2015.10.025.
[15] E.R. Horton, A. Byron, J.A. Askari, et al., Definition of a consensus integrin adhesome and its dynamics during adhesion complex assembly and disassembly, Nat. Cell Biol. 17 (12) (2015) 1577–1587, https://doi.org/10.1038/ncb3257.
[16] T.P. Lele, C.K. Thodeti, J. Pendse, D.E. Ingber, Investigating complexity of protein–protein interactions in focal adhesions, Biochem. Biophys. Res. Commun. 369 (3) (2008) 929–934, https://doi.org/10.1016/j.bbrc.2008.02.137.
[17] H. Wolfenson, A. Lubelski, T. Regev, J. Klafter, Y.I. Henis, B. Geiger, A role for the juxtamembrane cytoplasm in the molecular dynamics of focal adhesions, PLoS One 4 (1) (2009), e4304, https://doi.org/10.1371/journal.pone.0004304.
[18] J.-E. Hoffmann, Y. Fermin, R.L.O. Stricker, K. Ickstadt, E. Zamir, Symmetric exchange of multi-protein building blocks between stationary focal adhesions and the cytosol, Elife 3 (2014), e02257, https://doi.org/10.7554/eLife.02257. Singer RH, ed.
[19] B. Geiger, A. Bershadsky, Exploring the neighborhood: adhesion-coupled cell mechanosensors, Cell 110 (2) (2002) 139–142, https://doi.org/10.1016/S0092-8674(02)00831-0.
[20] D. Riveline, E. Zamir, N.Q. Balaban, et al., Focal contacts as mechanosensors: externally applied local mechanical force induces growth of focal contacts by an mDia1-dependent and ROCK-independent mechanism, J. Cell Biol. 153 (6) (2001) 1175–1185, https://doi.org/10.1083/jcb.153.6.1175.
[21] A.E. Miller, P. Hu, T.H. Barker, Feeling things out: bidirectional signaling of the cell–ECM interface, implications in the mechanobiology of cell spreading, migration, proliferation, and differentiation, Adv Healthc Mater 9 (8) (2020), https://doi.org/10.1002/adhm.201901445.
[22] K. Burridge, M. Chrzanowska-Wodnicka, Focal adhesions, contractility, and signaling, Annu. Rev. Cell Dev. Biol. 12 (1) (1996) 463–519, https://doi.org/10.1146/annurev.cellbio.12.1.463.
[23] B. Geiger, A. Bershadsky, R. Pankov, K.M. Yamada, Transmembrane extracellular matrix-cytoskeleton crosstalk, Nat. Rev. Mol. Cell Biol. 2 (11) (2001) 793–805, https://doi.org/10.1038/35099066.
[24] S.K. Mitra, D.A. Hanson, D.D. Schlaepfer, Focal adhesion kinase: in command and control of cell motility, Nat. Rev. Mol. Cell Biol. 6 (1) (2005) 56–68, https://doi.org/10.1038/nrm1549.
[25] M.P. Playford, M.D. Schaller, The interplay between Src and integrins in normal and tumor biology, Oncogene 23 (48 REV. ISS. 7) (2004) 7928–7946, https://doi.org/10.1038/sj.onc.1208080.
[26] J.T. Parsons, K.H. Martin, J.K. Slack, J.M. Taylor, S.A. Weed, Focal Adhesion Kinase: a regulator of focal adhesion dynamics and cell movement, Oncogene 19 (49) (2000) 5606–5613, https://doi.org/10.1038/sj.onc.1203877.
[27] D.J. Webb, J.T. Parsons, A.F. Horwitz, Adhesion assembly, disassembly and turnover in migrating cells – over and over and over again, Nat. Cell Biol. 4 (4) (2002) E97–E100, https://doi.org/10.1038/ncb0402-e97.
[28] J.T. Parsons, A.R. Horwitz, M.A. Schwartz, Cell adhesion: integrating cytoskeletal dynamics and cellular tension, Nat. Rev. Mol. Cell Biol. 11 (9) (2010) 633–643, https://doi.org/10.1038/nrm2957.
[29] S.M. Wahl, G.M. Feldman, J.B. McCarthy, Regulation of leukocyte adhesion and signaling in inflammation and disease, J. Leukoc. Biol. 59 (6) (1996) 789–796, https://doi.org/10.1002/jlb.59.6.789.
[30] T.A. Vahedi-Hunter, J.A. Estep, K.A. Rosette, M.L. Rutlin, K.M. Wright, M.M. Riccomagno, Cas adaptor proteins coordinate sensory axon fasciculation, Sci. Rep. 8 (1) (2018) 1–15, https://doi.org/10.1038/s41598-018-24261-x.
[31] M. Hagel, E.L. George, A. Kim, et al., The adaptor protein paxillin is essential for normal development in the mouse and is a critical transducer of fibronectin signaling, Mol. Cell Biol. 22 (3) (2002) 901–915, https://doi.org/10.1128/mcb.22.3.901-915.2002.
[32] W. Xu, H. Baribault, E.D. Adamson, Vinculin knockout results in heart and brain defects during embryonic development, Development 125 (2) (1998) 327–337, https://doi.org/10.1242/dev.125.2.327.
[33] S.J. Monkley, X.H. Zhou, S.J. Kinston, et al., Disruption of the talin gene arrests mouse development at the gastrulation stage, Dev Dyn an Off Publ Am Assoc Anat 219 (4) (2000) 560–574, https://doi.org/10.1002/1097-0177(2000)9999:9999. ::AID-DVDY1079>3.0.CO;2-Y.
[34] D. Ilić, Y. Furuta, S. Kanazawa, et al., Reduced cell motility and enhanced focal adhesion contact formation in cells from FAK-deficient mice, Nature 377 (6549) (1995) 539–544, https://doi.org/10.1038/377539A0.
[35] A. Bianchi-Smiraglia, S. Paesante, A.V. Bakin, Integrin β5 contributes to the tumorigenic potential of breast cancer cells through the Src-FAK and MEK-ERK signaling pathways, Oncogene 32 (25) (2013) 3049–3058, https://doi.org/10.1038/onc.2012.320.
[36] A.P. Maartens, N.H. Brown, The many faces of cell adhesion during Drosophila muscle development, Dev. Biol. 401 (1) (2015) 62–74, https://doi.org/10.1016/j.ydbio.2014.12.038.
[37] D. Bianconi, M. Unseld, G.W. Prager, Integrins in the spotlight of cancer, Int. J. Mol. Sci. 17 (12) (2016), https://doi.org/10.3390/ijms17122037.
[38] J.S. Desgrosellier, D.A. Cheresh, Integrins in cancer: biological implications and therapeutic opportunities, Nat. Rev. Cancer 10 (1) (2010) 9–22, https://doi.org/10.1038/nrc2748.
[39] F. Xu, J. Zhang, G. Hu, L. Liu, W. Liang, Hypoxia and TGF-β1 induced PLOD2 expression improve the migration and invasion of cervical cancer cells by promoting epithelial-to-mesenchymal transition (EMT) and focal adhesion formation, Cancer Cell Int. 17 (1) (2017) 54, https://doi.org/10.1186/s12935-017-0420-z.
[40] M.D. Schaller, C.A. Borgman, B.S. Cobb, R.R. Vines, A.B. Reynolds, J.T. Parsons, pp125(FAK), a structurally distinctive protein-tyrosine kinase associated with focal adhesions, Proc. Natl. Acad. Sci. U. S. A. 89 (11) (1992) 5192–5196, https://doi.org/10.1073/pnas.89.11.5192.
[41] L. Kornberg, H.S. Earp, J.T. Parsons, M. Schaller, R.L. Juliano, Cell adhesion or integrin clustering increases phosphorylation of a focal adhesion-associated tyrosine kinase, J. Biol. Chem. 267 (33) (1992) 23439–23442, https://doi.org/10.1016/s0021-9258(18)35853-8.
[42] S.K. Hanks, M.B. Calalb, M.C. Harper, S.K. Patel, Focal adhesion protein-tyrosine kinase phosphorylated in response to cell attachment to fibronectin, Proc. Natl. Acad. Sci. U. S. A. 89 (18) (1992) 8487–8491, https://doi.org/10.1073/pnas.89.18.8487.

[43] L. Lipfert, B. Haimovich, M.D. Schaller, B.S. Cobb, J.T. Parsons, J.S. Brugge, Integrin-dependent phosphorylation and activation of the protein tyrosine kinase pp125(FAK) in platelets, J. Cell Biol. 119 (4) (1992) 905–912, https://doi.org/10.1083/jcb.119.4.905.

[44] J.T. Parsons, Focal adhesion kinase: the first ten years, J. Cell Sci. 116 (8) (2003) 1409–1416, https://doi.org/10.1242/jcs.00373.

[45] J.L. Guan, J.E. Trevithick, R.O. Hynes, Fibronectin/integrin interaction induces tyrosine phosphorylation of a 120-kDa protein, Mol. Biol. Cell 2 (11) (1991) 951–964, https://doi.org/10.1091/mbc.2.11.951.

[46] L.J. Kornberg, H.S. Earp, C.E. Turner, C. Prockop, R.L. Juliano, Signal transduction by integrins: increased protein tyrosine phosphorylation caused by clustering of beta 1 integrins, Proc. Natl. Acad. Sci. USA 88 (19) (1991) 8392–8396, https://doi.org/10.1073/pnas.88.19.8392.

[47] C.R. Hauck, D.A. Hsia, D. Ilic, D.D. Schlaepfer, v-Src SH3-enhanced interaction with focal adhesion kinase at β1 integrin-containing invadopodia promotes cell invasion, J. Biol. Chem. 277 (15) (2002) 12487–12490, https://doi.org/10.1074/jbc.C100760200.

[48] N.R. Alexander, K.M. Branch, A. Parekh, et al., Extracellular matrix rigidity promotes invadopodia activity, Curr. Biol. 18 (17) (2008) 1295–1299, https://doi.org/10.1016/j.cub.2008.07.090.

[49] Y. Wang, M.A. McNiven, Invasive matrix degradation at focal adhesions occurs via protease recruitment by a FAK-p130Cas complex, J. Cell Biol. 196 (3) (2012) 375–385, https://doi.org/10.1083/jcb.201105153.

[50] K.T. Chan, C.L. Cortesio, A. Huttenlocher, Fak alters invadopodia and focal adhesion composition and dynamics to regulate breast cancer invasion, J. Cell Biol. 185 (2) (2009) 357–370, https://doi.org/10.1083/jcb.200809110.

[51] B.Y. Lee, P. Timpson, L.G. Horvath, R.J. Daly, FAK signaling in human cancer as a target for therapeutics, Pharmacol. Ther. 146 (2015) 132–149, https://doi.org/10.1016/j.pharmthera.2014.10.001.

[52] F.J. Sulzmaier, C. Jean, D.D. Schlaepfer, FAK in cancer: mechanistic findings and clinical applications, Nat. Rev. Cancer 14 (9) (2014) 598–610, https://doi.org/10.1038/nrc3792.

[53] X. Feng, N. Arang, D.C. Rigiracciolo, et al., A platform of synthetic lethal gene interaction networks reveals that the GNAQ uveal melanoma oncogene controls the hippo pathway through FAK, Cancer Cell 35 (3) (2019) 457, https://doi.org/10.1016/j.ccell.2019.01.009, 472.e5.

[54] Y.H. Kim, H.K. Kim, H.Y. Kim, et al., FAK-copy-gain is a predictive marker for sensitivity to fak inhibition in breast cancer, Cancers 11 (9) (2019) 1–14, https://doi.org/10.3390/cancers11091288.

[55] M. Agochiya, V.G. Brunton, D.W. Owens, et al., Increased dosage and amplification of the focal adhesion kinase gene in human cancer cells, Oncogene 18 (41) (1999) 5646–5653, https://doi.org/10.1038/sj.onc.1202957, 1999 1841.

[56] P.P. Provenzano, P.J. Keely, The role of focal adhesion kinase in tumor initiation and progression, Cell Adhes. Migrat. 3 (4) (2009) 1–5, https://doi.org/10.4161/cam.3.4.9458.

[57] X.D. Ren, W.B. Kiosses, D.J. Sieg, C.A. Otey, D.D. Schlaepfer, M.A. Schwartz, Focal adhesion kinase suppresses Rho activity to promote focal adhesion, J. Cell Sci. 113 (20) (2000) 3673–3678.

[58] B.H. Chen, J.T.C. Tzen, A.R. Bresnick, H. Chen, Roles of Rho-associated kinase and myosin light chain kinase in morphological and migratory defects of focal adhesion kinase-null cells, J. Biol. Chem. 277 (37) (2002) 33857–33863, https://doi.org/10.1074/jbc.M204429200.

[59] D.J. Sieg, C.R. Hauck, D.D. Schlaepfer, Required role of focal adhesion kinase (FAK) for integrin-stimulated cell migration, J. Cell Sci. 112 (16) (1999) 2677–2691.

[60] D.J. Webb, K. Donais, L.A. Whitmore, et al., FAK-Src signalling through paxillin, ERK and MLCK regulates adhesion disassembly, Nat. Cell Biol. 6 (2) (2004) 154–161, https://doi.org/10.1038/ncb1094.

[61] M.D. Schaller, J.D. Hildebrand, J.D. Shannon, J.W. Fox, R.R. Vines, J.T. Parsons, Autophosphorylation of the focal adhesion kinase, pp125FAK, directs SH2-dependent binding of pp60src, Mol. Cell Biol. 14 (3) (1994) 1680–1688, https://doi.org/10.1128/MCB.14.3.1680-1688.1994.

[62] I. Acebrón, R.D. Righetto, C. Schoenherr, et al., Structural basis of Focal Adhesion Kinase activation on lipid membranes, EMBO J. 39 (19) (2020) 1–21, https://doi.org/10.15252/embj.2020104743.

[63] J.L. Guan, D. Shalloway, Regulation of focal adhesion-associated protein tyrosine kinase by both cellular adhesion and oncogenic transformation, Nature 358 (6388) (1992) 690–692, https://doi.org/10.1038/358690a0.

[64] K. Brami-Cherrier, N. Gervasi, D. Arsenieva, et al., FAK dimerization controls its kinase-dependent functions at focal adhesions, EMBO J. 33 (4) (2014) 356–370, https://doi.org/10.1002/embj.201386399.

[65] F. Brod, R. Fässler, A FAK conundrum is solved: activation and organization of focal adhesion kinase at the plasma membrane, EMBO J. 39 (19) (2020) 1–3, https://doi.org/10.15252/embj.2020106234.

[66] M.B. Calalb, T.R. Polte, S.K. Hanks, Tyrosine phosphorylation of focal adhesion kinase at sites in the catalytic domain regulates kinase activity: a role for Src family kinases, Mol. Cell Biol. 15 (2) (1995) 954–963, https://doi.org/10.1128/MCB.15.2.954.

[67] Z. Xing, H.C. Chen, J.K. Nowlen, S.J. Taylor, D. Shalloway, J.L. Guan, Direct interaction of v-Src with the focal adhesion kinase mediated by the Src SH2 domain, Mol. Biol. Cell 5 (4) (1994) 413–421, https://doi.org/10.1091/mbc.5.4.413.

[68] B.S. Cobb, M.D. Schaller, T.H. Leu, J.T. Parsons, Stable association of pp60src and pp59fyn with the focal adhesion-associated protein tyrosine kinase, pp125FAK, Mol. Cell Biol. 14 (1) (1994) 147–155, https://doi.org/10.1128/mcb.14.1.147-155.1994.

[69] B.L. Eide, C.W. Turck, J.A. Escobedo, Identification of Tyr-397 as the primary site of tyrosine phosphorylation and pp60src association in the focal adhesion kinase, pp125FAK, Mol. Cell Biol. 15 (5) (1995) 2819–2827, https://doi.org/10.1128/MCB.15.5.2819.

[70] R. Zaidel-Bar, C. Ballestrem, Z. Kam, B. Geiger, Early molecular events in the assembly of matrix adhesions at the leading edge of migrating cells, J. Cell Sci. 116 (22) (2003) 4605–4613, https://doi.org/10.1242/jcs.00792.

[71] D.J. Webb, C.M. Brown, A.F. Horwitz, Illuminating adhesion complexes in migrating cells: moving toward a bright future, Curr. Opin. Cell Biol. 15 (5) (2003) 614–620, https://doi.org/10.1016/S0955-0674(03)00105-4.

[72] A. Hamadi, M. Bouali, M. Dontenwill, H. Stoeckel, K. Takeda, P. Rondé, Regulation of focal adhesion dynamics and disassembly by phosphorylation of FAK at tyrosine 397, J. Cell Sci. 118 (19) (2005) 4415–4425, https://doi.org/10.1242/jcs.02565.

[73] J.D. Owen, P.J. Ruest, D.W. Fry, S.K. Hanks, Induced focal adhesion kinase (FAK) expression in FAK-null cells enhances cell spreading and migration requiring both auto- and activation loop phosphorylation sites and inhibits adhesion-dependent tyrosine phosphorylation of Pyk2, Mol. Cell Biol. 19 (7) (1999) 4806–4818, https://doi.org/10.1128/mcb.19.7.4806.

[74] P.J. Ruest, S. Roy, E. Shi, R.L. Mernaugh, S.K. Hanks, Phosphospecific antibodies reveal focal adhesion kinase activation loop phosphorylation in nascent and mature focal adhesions and requirement for the autophosphorylation site, Cell growth Differ Mol Biol J Am Assoc Cancer Res 11 (1) (2000) 41–48.

[75] D. Lietha, X. Cai, D.F.J. Ceccarelli, Y. Li, M.D. Schaller, M.J. Eck, Structural basis for the autoinhibition of focal adhesion kinase, Cell 129 (6) (2007) 1177–1187, https://doi.org/10.1016/j.cell.2007.05.041.

[76] X. Cai, D. Lietha, D.F. Ceccarelli, et al., Spatial and temporal regulation of focal adhesion kinase activity in living cells, Mol. Cell Biol. 28 (1) (2008) 201–214, https://doi.org/10.1128/mcb.01324-07.

[77] J.M. Dunty, M.D. Schaller, The N termini of focal adhesion kinase family members regulate substrate phosphorylation, localization, and cell morphology, J. Biol. Chem. 277 (47) (2002) 45644–45654, https://doi.org/10.1074/jbc.M201779200.

[78] J.M. Dunty, V. Gabarra-Niecko, M.L. King, D.F.J. Ceccarelli, M.J. Eck, M.D. Schaller, FERM domain interaction promotes FAK signaling, Mol. Cell Biol. 24 (12) (2004) 5353–5368, https://doi.org/10.1128/mcb.24.12.5353-5368.2004.

[79] M.B. Calalb, T.R. Polte, S.K. Hanks, Tyrosine phosphorylation of focal adhesion kinase at sites in the catalytic domain regulates kinase activity: a role for Src family kinases, Mol. Cell Biol. 15 (2) (1995) 954–963, https://doi.org/10.1128/mcb.15.2.954.

[80] P. Nollau, B.J. Mayer, Profiling the global tyrosine phosphorylation state by Src homology 2 domain binding, Proc. Natl. Acad. Sci. U. S. A. 98 (24) (2001) 13531–13536, https://doi.org/10.1073/pnas.241215998.

[81] G. Giannone, P. Rondé, M. Gaire, J. Haiech, K. Takeda, Calcium oscillations trigger focal adhesion disassembly in human U87 astrocytoma cells, J. Biol. Chem. 277 (29) (2002) 26364–26371, https://doi.org/10.1074/jbc.M203952200.

[82] J. Kirchner, Z. Kam, G. Tzur, A.D. Bershadsky, B. Geiger, Live-cell monitoring of tyrosine phosphorylation in focal adhesions following microtubule disruption, J. Cell Sci. 116 (6) (2003) 975–986, https://doi.org/10.1242/jcs.00284.

[83] M. De Virgilio, W.B. Kiosses, S.J. Shattil, Proximal, selective, and dynamic interactions between integrin αIIbβ3 and protein tyrosine kinases in living cells, J. Cell Biol. 165 (3) (2004) 305–311, https://doi.org/10.1083/jcb.200402064.

[84] E. Papusheva, F.M. de Queiroz, J. Dalous, et al., Dynamic conformational changes in the FERM domain of FAK are involved in focal-adhesion behavior during cell spreading and motility, J. Cell Sci. 122 (5) (2009) 656–666, https://doi.org/10.1242/jcs.028738.

[85] J. Seong, M. Ouyang, T. Kim, et al., Detection of focal adhesion kinase activation at membrane microdomains by fluorescence resonance energy transfer, Nat. Commun. 2 (1) (2011), https://doi.org/10.1038/ncomms1414.

[86] M. Ritt, J.L. Guan, S. Sivaramakrishnan, Visualizing and manipulating Focal Adhesion Kinase regulation in live cells, J. Biol. Chem. 288 (13) (2013) 8875–8886, https://doi.org/10.1074/jbc.M112.421164.

[87] E.R. Horton, J.D. Humphries, B. Stutchbury, et al., Modulation of FAK and Src adhesion signaling occurs independently of adhesion complex composition, J. Cell Biol. 212 (3) (2016) 349–364, https://doi.org/10.1083/jcb.201508080.

[88] Y. Wu, K. Zhang, J. Seong, et al., In-situ coupling between kinase activities and protein dynamics within single focal adhesions, Sci. Rep. (2016;6(February) 1–13, https://doi.org/10.1038/srep29377.

[89] N.P. Damayanti, K. Buno, N. Narayanan, S.L. Voytik Harbin, M. Deng, J.M.K. Irudayaraj, Monitoring focal adhesion kinase phosphorylation dynamics in live cells, Analyst 142 (15) (2017) 2713–2716, https://doi.org/10.1039/c7an00471k.

[90] F. Rossi, C.A. Charlton, H.M. Blau, Monitoring protein-protein interactions in intact eukaryotic cells by β-galactosidase complementation, Proc. Natl. Acad. Sci. U. S. A. 94 (16) (1997) 8405–8410, https://doi.org/10.1073/pnas.94.16.8405.

[91] I. Remy, A. Galarneau, S.W. Michnick, Detection and visualization of protein interactions with protein fragment complementation assays, Methods Mol. Biol. 185 (2002) 447–459, https://doi.org/10.1385/1-59259-241-4:447.

[92] T.K. Kerppola, Bimolecular fluorescence complementation (BiFC) analysis as a probe of protein interactions in living cells, Annu. Rev. Biophys. 37 (1) (2008) 465–487, https://doi.org/10.1146/annurev.biophys.37.032807.125842.

[93] C.D. Hu, T.K. Kerppola, Simultaneous visualization of multiple protein interactions in living cells using multicolor fluorescence complementation analysis, Nat. Biotechnol. 21 (5) (2003) 539–545, https://doi.org/10.1038/nbt816.

[94] K.E. Luker, M.C.P. Smith, G.D. Luker, S.T. Gammon, H. Piwnica-Worms, D. Piwnica-Worms, Kinetics of regulated protein-protein interactions revealed with firefly luciferase complementation imaging in cells and living animals, Proc. Natl. Acad. Sci. U. S. A. 101 (33) (2004) 12288–12293, https://doi.org/10.1073/pnas.0404041101.

[95] T. Azad, A. Tashakor, S. Hosseinkhani, Split-luciferase complementary assay: applications, recent developments, and future perspectives, Anal. Bioanal. Chem. 406 (23) (2014) 5541–5560, https://doi.org/10.1007/s00216-014-7980-8.

[96] M.C. Lake, E.O. Aboagye, Luciferase fragment complementation imaging in preclinical cancer studies, Oncoscience 1 (5) (2014) 310–325, https://doi.org/10.18632/oncoscience.45.

[97] C. Ballestrem, N. Erez, J. Kirchner, Z. Kam, A. Bershadsky, B. Geiger, Molecular mapping of tyrosine-phosphorylated proteins in focal adhesion using fluorescence resonance energy transfer, J. Cell Sci. 119 (5) (2006) 866–875, https://doi.org/10.1242/jcs.02794.

[98] V.V. Iyer, C. Ballestrem, J. Kirchner, B. Geiger, M.D. Schaller, Measurement of protein tyrosine phosphorylation in cell adhesion, Methods Mol. Biol. 294 (2005) 289–302, https://doi.org/10.1385/1-59259-860-9:289.

[99] J.J. Lee, R.A.H. van de Ven, E. Zaganjor, et al., Inhibition of epithelial cell migration and Src/FAK signaling by SIRT3, Proc. Natl. Acad. Sci. USA 115 (27) (2018) 7057–7062, https://doi.org/10.1073/pnas.1800440115.

[100] A. Koenig, C. Mueller, C. Hasel, G. Adler, A. Menke, Collagen type I induces disruption of E-cadherin-mediated cell-cell contacts and promotes proliferation of pancreatic carcinoma cells, Cancer Res. 66 (9) (2006) 4662–4671, https://doi.org/10.1158/0008-5472.CAN-05-2804.

[101] J.C. Juárez-Cruz, M.D. Zuñiga-Eulogio, M. Olea-Flores, et al., Leptin induces cell migration and invasion in a FAK-Src-dependent manner in breast cancer cells, Endocr Connect 8 (11) (2019) 1539–1552, https://doi.org/10.1530/EC-19-0442.

[102] F. Pontén, K. Jirström, M. Uhlen, The human protein atlas—a tool for pathology, J. Pathol. 216 (4) (2008) 387–393, https://doi.org/10.1002/path.2440.

[103] D.L. Mendrick, D.M. Kelly, Temporal expression of VLA-2 and modulation of its ligand specificity by rat glomerular epithelial cells in vitro, Lab. Invest. 69 (6) (1993) 690–702.

[104] E. Zamir, M. Katz, Y. Posen, et al., Dynamics and segregation of cell-matrix adhesions in cultured fibroblasts, Nat. Cell Biol. 2 (4) (2000) 191–196, https://doi.org/10.1038/35008607.

[105] K. Burridge, C.E. Turner, L.H. Romer, Tyrosine phosphorylation of paxillin and pp125FAK accompanies cell adhesion to extracellular matrix: a role in cytoskeletal assembly, J. Cell Biol. 119 (4) (1992) 893–903, https://doi.org/10.1083/jcb.119.4.893.

[106] J.T. Parsons, Focal adhesion kinase: the first ten years, J. Cell Sci. 116 (Pt 8) (2003) 1409–1416, https://doi.org/10.1242/JCS.00373.

[107] J. Wu, Y. Chen, C. Kuo, et al., Focal adhesion kinase-dependent focal adhesion recruitment of SH2 domains directs SRC into focal adhesions to regulate cell adhesion and migration, Nat Publ Gr (2015;(December) 1–13, https://doi.org/10.1038/srep18476.

[108] J.D. Humphries, P. Wang, C. Streuli, B. Geiger, M.J. Humphries, C. Ballestrem, Vinculin controls focal adhesion formation by direct interactions with talin and actin, J. Cell Biol. 179 (5) (2007) 1043–1057, https://doi.org/10.1083/jcb.200703036.

[109] J.P. Myers, T.M. Gomez, Focal adhesion kinase promotes integrin adhesion dynamics necessary for chemotropic turning of nerve growth cones, J. Neurosci. 31 (38) (2011) 13585–13595, https://doi.org/10.1523/JNEUROSCI.2381-11.2011.

[110] M. Felkl, K. Tomas, M. Smid, J. Mattes, R. Windoffer, R.E. Leube, Monitoring the cytoskeletal EGF response in live gastric carcinoma cells, PLoS One 7 (9) (2012), e45280, https://doi.org/10.1371/journal.pone.0045280.

[111] W. Guo, Y. Wang, Retrograde fluxes of focal adhesion proteins in response to cell migration and mechanical signals, Mol. Biol. Cell 18 (11) (2007) 4519–4527, https://doi.org/10.1091/mbc.e07-06-0582.

[112] A.J. McKenzie, K.V. Svec, T.F. Williams, A.K. Howe, Protein kinase A activity is regulated by actomyosin contractility during cell migration and is required for durotaxis, Mol. Biol. Cell 31 (1) (2019) 45–58, https://doi.org/10.1091/mbc.E19-03-0131.

[113] J.S. Logue, A.X. Cartagena-Rivera, R.S. Chadwick, c-Src activity is differentially required by cancer cell motility modes, Oncogene 37 (16) (2018) 2104–2121, https://doi.org/10.1038/s41388-017-0071-5.

[114] K.E. Kubow, S.K. Conrad, A.R. Horwitz, Matrix microarchitecture and myosin II determine adhesion in 3D matrices, Curr. Biol. 23 (17) (2013) 1607–1619, https://doi.org/10.1016/j.cub.2013.06.053.

[115] M. Santiago-Medina, J.P. Myers, T.M. Gomez, Imaging adhesion and signaling dynamics in Xenopus laevis growth cones, Dev Neurobiol 72 (4) (2012) 585–599, https://doi.org/10.1002/dneu.20886.

[116] T.K. Kerppola, Visualization of molecular interactions using bimolecular fluorescence complementation analysis: characteristics of protein fragment complementation, Chem. Soc. Rev. 38 (10) (2009) 2876–2886, https://doi.org/10.1039/b909638h.

[117] M.D. Schaller, C.A. Borgman, B.S. Cobb, R.R. Vines, A.B. Reynolds, J.T. Parsons, pp125FAK a structurally distinctive protein-tyrosine kinase associated with focal adhesions, Proc. Natl. Acad. Sci. U. S. A. 89 (11) (1992) 5192–5196, https://doi.org/10.1073/PNAS.89.11.5192.

[118] M.A. Westhoff, B. Serrels, V.J. Fincham, M.C. Frame, N.O. Carragher, Src-mediated phosphorylation of focal adhesion kinase couples actin and adhesion dynamics to survival signaling, Mol. Cell Biol. 24 (18) (2004) 8113–8133, https://doi.org/10.1128/mcb.24.18.8113-8133.2004.

[119] D.J. Webb, K. Donais, L.A. Whitmore, et al., FAK-Src signalling through paxillin, ERK and MLCK regulates adhesion disassembly, Nat. Cell Biol. 6 (2) (2004) 154–161, https://doi.org/10.1038/ncb1094.

[120] R. Paulmurugant, S.S. Gambhir, Monitoring protein-protein interactions using split synthetic renilla luciferase protein-fragment-assisted complementation, Anal. Chem. 75 (7) (2003) 1584–1589, https://doi.org/10.1021/ac020731c.

[121] I. Remy, S.W. Michnick, A highly sensitive protein-protein interaction assay based on Gaussia luciferase, Nat. Methods 3 (12) (2006) 977–979, https://doi.org/10.1038/nmeth979.

[122] V. Villalobos, S. Naik, M. Bruinsma, et al., Dual-color click beetle luciferase heteroprotein fragment complementation assays, Chem. Biol. 17 (9) (2010) 1018–1029, https://doi.org/10.1016/j.chembiol.2010.06.018.
[123] E. Stefan, S. Aquin, N. Berger, et al., Quantification of dynamic protein complexes using Renilla luciferase fragment complementation applied to protein kinase A activities in vivo, Proc. Natl. Acad. Sci. U. S. A. 104 (43) (2007) 16916–16921, https://doi.org/10.1073/pnas.0704257104.
[124] L.A. Cohen, J.-L. Guan, Residues within the first subdomain of the FERM-like domain in focal adhesion kinase are important in its regulation, J. Biol. Chem. 280 (9) (2005) 8197–8207, https://doi.org/10.1074/jbc.M412021200.
[125] D. Lietha, X. Cai, D.F.J. Ceccarelli, Y. Li, M.D. Schaller, M.J. Eck, Structural basis for the autoinhibition of focal adhesion kinase, Cell 129 (6) (2007) 1177, https://doi.org/10.1016/J.CELL.2007.05.041.
[126] R. Paulmurugan, S.S. Gambhir, Combinatorial library screening for developing an improved split-firefly luciferase fragment-assisted complementation system for studying protein-protein interactions, Anal. Chem. 79 (6) (2007) 2346–2353, https://doi.org/10.1021/ac062053q.
[127] S. Liu, Y. Su, M.Z. Lin, J.A. Ronald, Brightening up biology: advances in luciferase systems for in vivo imaging, ACS Chem. Biol. 16 (12) (2021) 2707–2718, https://doi.org/10.1021/acschembio.1c00549.
[128] H.-H. Chuang, Y. Zhen, Y. Tsai, et al., FAK in cancer: from mechanisms to therapeutic strategies, Int. J. Mol. Sci. 23 (3) (2022) 1726, https://doi.org/10.3390/ijms23031726.
[129] J.C. Dawson, A. Serrels, D.G. Stupack, D.D. Schlaepfer, M.C. Frame, Targeting FAK in anticancer combination therapies, Nat. Rev. Cancer 21 (5) (2021) 313–324, https://doi.org/10.1038/s41568-021-00340-6.
[130] J.M. Murphy, Y.A.R. Rodriguez, K. Jeong, E.Y.E. Ahn, S.T.S. Lim, Targeting focal adhesion kinase in cancer cells and the tumor microenvironment, Exp. Mol. Med. 52 (6) (2020) 877–886, https://doi.org/10.1038/s12276-020-0447-4.
[131] A. Chauhan, T. Khan, Focal adhesion kinase—an emerging viable target in cancer and development of focal adhesion kinase inhibitors, Chem. Biol. Drug Des. 97 (3) (2021) 774–794, https://doi.org/10.1111/cbdd.13808.
[132] D.C. Rigiracciolo, F. Cirillo, M. Talia, et al., Focal adhesion kinase fine tunes multifaced signals toward breast cancer progression, Cancers 13 (4) (2021) 1–29, https://doi.org/10.3390/cancers13040645.
[133] Y. Zhang, S. Liu, S. Zhou, et al., Focal adhesion kinase: insight into its roles and therapeutic potential in oesophageal cancer, Cancer Lett. 496 (October 2020) (2021) 93–103, https://doi.org/10.1016/j.canlet.2020.10.005.
[134] R. Kanteti, T. Mirzapoiazova, J.J. Riehm, I. Dhanasingh, B. Mambetsariev, J. Wang, Focal adhesion kinase a potential therapeutic target for pancreatic cancer and malignant pleural mesothelioma, Cancer Biol. Ther. 19 (4) (2018) 316–327, https://doi.org/10.1080/15384047.2017.1416937.
[135] M.A. Zakaria, N.F. Rajab, E.W. Chua, G.T. Selvarajah, S.F. Masre, The roles of tissue rigidity and its underlying mechanisms in promoting tumor growth, Cancer Invest. 38 (8–9) (2020) 445–462, https://doi.org/10.1080/07357907.2020.1802474.
[136] C.R. Hauck, D.A. Hsia, D.D. Schlaepfer, The focal adhesion kinase—a regulator of cell migration and invasion structural characteristics of FAK-like protein tyrosine kinases focal adhesion kinase (FAK) 1 together with pyk2 (1) form a subfamily of FAK-like protein-tyrosine kinases (PTKs), FAK. *IUBMB Life*. 53 (2002) 115–119, https://doi.org/10.1080/10399710290039007.
[137] Y. Wu, N. Li, C. Ye, et al., Focal adhesion kinase inhibitors, a heavy punch to cancer, Discov Oncol 12 (1) (2021), https://doi.org/10.1007/s12672-021-00449-y.
[138] I. Antoniades, M. Kyriakou, A. Charalambous, et al., FAK displacement from focal adhesions: a promising strategy to target processes implicated in cancer progression and metastasis, Cell Commun. Signal. 19 (1) (2021) 3, https://doi.org/10.1186/s12964-020-00671-1.
[139] X.-J. Pang, X.-J. Liu, Y. Liu, et al., Drug discovery targeting focal adhesion kinase (FAK) as a promising cancer therapy, Molbank 26 (14) (2021), https://doi.org/10.3390/molecules26144250.
[140] A. Mousson, E. Sick, P. Carl, D. Dujardin, J. De Mey, P. Rondé, Targeting focal adhesion kinase using inhibitors of protein-protein interactions, Cancers 10 (9) (2018) 1–29, https://doi.org/10.3390/cancers10090278.